Structural Engineering and Mechanics, Vol. 39, No. 4 (2011) 465-498
DOI: http://dx.doi.org/10.12989/sem.2011.39.4.465

Bilinear elastodynamical models of cracked concrete beams

Umesh Kumar Pandey*[1] and Gurmail S. Benipal[2a]

[1]*Department of Civil Engineering, National Institute of Technology, Hamirpur (H.P.)-177005, India*
[2]*Department of Civil Engineering, Indian Institute of Technology Delhi, Hauz Khas, New Delhi-110016, India*

(Received February 16, 2010, Accepted May 25, 2011)

Abstract. Concrete structures are generally cracked in flexural tension at working loads. Concrete beams with asymmetric section details and crack patterns exhibit different flexural rigidity depending upon the sense of the applied flexural moment. In this paper, three different models, having the same natural period, of such SDOF bilinear dynamical systems have been proposed. The Model-I and Model-II have constant damping coefficient, but the latter is characterized by two stiffness coefficients depending upon the sense of vibration amplitude. The Model-III, additionally, has two damping coefficients as well. In this paper, the dynamical response of Model-III to sinusoidal loading has been investigated and compared with that of Model-II studied earlier. It has been found that Model-III exhibits regular and irregular sub-harmonics, jump phenomena and strong sensitivity to initial conditions, forcing frequency, system period as well as the sense of peak sinusoidal force. The constant sustained load has been found to affect the natural period of the dynamical system. The predictions of Model-I have been compared with those of the approximate linear model adopted in present practice. The behaviour exhibited by different models of the SDOF cracked elastic concrete structures under working loads and the theoretical and practical implications of the approach followed have been critically evaluated.

Keywords: bilinear dynamics; bilinearity ratio; cracked concrete structures; jump phenomena; sensitivity to system parameters; stability portrait; sub-harmonic resonance

1. Introduction

In spite of the other types of dynamic loading, the discipline of dynamics of concrete structures is mainly informed by the demands of their seismic design. As per the contemporary design practice, the seismic analysis methods presume the concrete structures to be linear elastic. The member stiffness values are computed in reference to the gross section without recognizing the presence of reinforcement and cracking. One of the methods of determining the elastic dynamic response to an earthquake involves the use of elastic response spectrum. The elastic response of concrete structures so determined is then modified by using the response reduction coefficient (Agarwal and Shrikhande 2006, IS-1893 2002, Pauley and Priestley 1982, Penelis and Kappos 1997) in view of

*Corresponding author, Assistant Professor, E-mail: ukp@nitham.ac.in, ukp8@rediffmail.com
[a]Associate Professor, E-mail: gurmail@civil.iitd.ac.in

their elasto-plastic behaviour. However, under the action of earthquakes of magnitude lower than the design earthquake, the concrete structures do not exhibit such elasto-plastic behavior. In these cases, their elastodynamic response has to be determined and elastic response spectra have to be constructed for seismic design purposes. Such dynamic analysis is also expected to be useful for other dynamic loads like those due to wind, rotating machinery, etc.

In comparison to the very large number of research investigations relevant to seismic design, there is paucity of available literature dealing with the intrinsic dynamical behavior of concrete structures. Some impetus for investigating the effect of cracking on their dynamical behavior has been provided by the need for dynamic system identification of damaged concrete structures required for their structural health monitoring. The most popular experimental methodology adopted involves subjecting the concrete beams to increasing levels of damage loads in discrete steps. After unloading at each damage level, the beam is excited into free vibrations by impact hammer or subjected to harmonic forcing function. The response waveforms obtained are analyzed by quite sophisticated analytical methods like Hilbert-Huang transformation (Zhu and Law 2007) and wavelet transform (Carrión *et al.* 2006).

There exists considerable empirical evidence indicating the amplitude-dependence of the vibration frequency of cracked concrete beams. This fact has been interpreted to imply that cracked concrete beams exhibit nonlinear dynamical response. It has been found that the change in dependence of fundamental frequency on vibration amplitude is the greatest at low damage levels and decreases with increase in damage level. It has also been found that the extent of damage suffered by the concrete beams due to prior loading does not affect the mode shapes, but only the modal frequency and modal damping. As expected, modal frequencies decrease whereas modal damping ratios increase with damage level (Wang *et al*. 1998, Eccles *et al*. 1999, Ndambi *et al*. 2000, Neild *et al*. 2003, Bayissa and Haritos 2004, Salzman *et al*. 2003, Newtson *et al*. 2006, Teguh *et al*. 2006, Musial *et al*. 2009, Zhu *et al*. 2009).

The modal frequencies for T-beams with ‘closed’ cracks under self-weight are expected to be higher than those for the ‘open’ cracks under higher damage loads and modal frequencies for the ‘breathing’ cracks (closing and reopening cracks) under lesser damage load are expected to lie between the above two extreme values. However, the experimental data is found to be incompatible with these expectations. For example, the breathing - crack condition has been found to exhibit the lowest frequency for the first mode. Also, the concrete beam in the breathing crack condition has been observed to exhibit the presence of higher frequency harmonics as well. No possible cause for such irregular dynamical behavior has been put forward (Bayissa and Haritos 2004).

Harmonically forced cracked concrete beams have been modeled as a softening Duffing oscillator and predicted to exhibit jump phenomenon. In nonlinear dynamical systems theory, the characteristic jump phenomenon refers to the distinct unstable response under increasing and decreasing forcing frequency. The model predictions have been satisfactorily validated with experimental data. For concrete beams damaged to higher extent by pre-loading, the difference between frequency domain response under increasing and decreasing forcing frequency has been observed to be more (Chen *et al*. 2006).

Under the action of working loads, the concrete structures are invariably cracked in flexural tension. Even though the formation and development of these cracks introduces nonlinearity and inelasticity, the behavior of concrete structures remains nonlinear elastic during the closing and reopening of the existing cracks caused by the variations of service loads. Due to the discrete nature of the cracks and the low yet finite tensile strength of concrete, the determination of the member stiffness must incorporate the tension stiffening effect. The need to incorporate the complexities associated with inelasticity and tension stiffening into structural analysis is obviated by assuming the concrete to be a no-tension solid. A statical theory of such nonlinear elastic concrete structures has been proposed by Benipal (1994). It has been shown that these structures belong to the class of homogeneous mechanical systems.

Under the action of single loads as well as during proportional load variations, such structures exhibit bilinear elastic response. This is due to the fact that the system stiffness values depend on the sense of the applied loads. For example, the flexural rigidity values for a beam with different top and bottom reinforcement under positive and negative flexural moments are different. Typical range of the values of the bilinearity ratio ---the ratio of the negative displacement stiffness to positive displacement stiffness ---for various types of reinforced concrete beams has been established (Pandey and Benipal 2006, Pandey 2008). It has been found that the maximum value of the bilinearity ratio is around 10 for fully cracked rectangular concrete beams with maximum bottom reinforcement (4%) and minimum top reinforcement (0.2%). Such a bilinearity differs from the one associated with elasto-plastic response mentioned above as, in the present case, it refers to the discontinuity at origin in their elastic moment-curvature and load-displacement curves. Others have also recognized the above mentioned dependence of the section flexural rigidity upon the sign of the applied flexural moment. However, the presence of experimentally observed subharmonics in the frequency domain response has not been predicted by the proposed model (Huszar 2008). It is argued here that SDOF cracked concrete beam should be modeled as a bilinear dynamical system, not as a softening Duffing oscillator as attempted by some researchers (Chen *et al*. 2006).

Dynamical behavior of such bilinear elastic SDOF concrete structures has recently been studied by the authors (Pandey and Benipal 2006, Pandey 2008). Such structures have been shown to exhibit both regular and irregular sub-harmonic resonances, strong dependence of steady state response on the initial conditions, bifurcations and chaotic motions even under sinusoidal loading. Adopting the approach followed by Thompson and coworkers (Thompson *et al*. 1983, Thompson *et al*. 1984, Thompson and Elvey 1984, Thompson and Stewart 1986), in the above study, the mass as well as the damping coefficient of the structure has been assumed to be constant whereas the stiffness coefficient has been assigned different values depending upon the sense of the vibration amplitude. Such a dynamical system has been called Model-II in the present study. The value of the damping coefficient has been determined from an averaged stiffness coefficient yielding the same period as the actual bilinear system. Obviously, the mass of the vibrating system being constant, two values of critical damping could be determined corresponding to the two values of stiffness. Assumption of the constant damping coefficient implies different values of damping ratio depending upon the sense of the amplitude. In view of this fact, in some cases, the concrete structures have been shown to execute overdamped and underdamped free vibrations respectively for positive and negative amplitudes as initial conditions.

It is well known, however, that the mechanical systems are not characterized by their damping coefficients but by their damping ratios. For example, steel and concrete structures are known to have damping ratios equal to about two and five percent respectively (IS-1893 2002). In the conventional SDOF systems, the damping coefficient is determined from their characteristic damping ratio and the critical damping coefficient. For the case of MDOF systems with Rayleigh damping---a special case of classical damping---the damping matrix turns out to be a linear function of the mass matrix and the stiffness matrix. The modal damping ratios are found to depend on the corresponding modal frequencies. In contrast, even the SDOF bilinear systems exhibit two values of the stiffness. In the earlier paper (Pandey and Benipal 2006), the damping coefficient for such bilinear concrete structures has been determined as a single value for the entire vibration cycle from the averaged stiffness and the damping ratio. However, depending upon the sense of displacement and the corresponding value of the stiffness, the same damping ratio implies two different values of damping coefficient. Thus, there exist two types of dynamical models of bilinear systems with two values of stiffness: one with single value (Model-II) and another with two values (Model-III) of damping coefficient. The available literature is silent about the relative merits of these two models of cracked concrete structures.

For simplicity of analysis, an equivalent unilinear model (Model-I) of the actual bilinear dynamical systems can be envisaged. Its stiffness value corresponds to the above mentioned averaged stiffness value independent of the sense of the vibration amplitude. Linear elastic dynamic analysis conducted based on the above assumption is expected to be more relevant for cracked reinforced concrete structures than the current approach based on gross stiffness determined from the assumption of uncracked and unreinforced concrete structures. All these models of SDOF bilinear dynamical systems have the same natural frequency and period.

In this paper, the dynamical response of cracked concrete structures modeled as bilinear SDOF dynamical systems has been studied. In particular, the dynamical behaviour of Model-I and Model-III subjected to sinusoidal loading has been investigated by using the techniques of nonlinear dynamical systems theory. The predicted time domain and frequency domain response has been compared with that of Model-II obtained earlier (Pandey and Benipal 2006) and the approximate analytical method currently followed in practice. The effect of constant sustained load on such dynamical response of the system has also been determined. The results obtained and the approach followed in this paper has been critically evaluated. The scope of the present investigation is restricted to cracked reinforced concrete structures under working loads undergoing only small deformations. Unless otherwise specified, the dynamic response has been computed for the bilinearity ratio of eight and the damping ratio of five percent. As in the case of other well known nonlinear dynamical systems like Duffing oscillator, van der Pol oscillator, etc., the scope of the present investigation is restricted to lumped mass SDOF systems.

2. Bilinear elastodynamics

Consider an SDOF bilinear mechanical system with lumped mass m, the bilinearity ratio β and the damping ratio ξ. The stiffness values for the positive and negative displacements are k_1 and k_2 respectively. The natural time period for the complete vibration cycle is T, which equals the average value of the time periods T_1 and T_2 corresponding to the stiffness coefficients k_1 and k_2 respectively. Thus

$$T = \frac{1}{2}(T_1 + T_2), \quad T_1 = 2\pi\sqrt{\left(\frac{m}{k_1}\right)} \quad \text{and} \quad T_2 = 2\pi\sqrt{\left(\frac{m}{k_2}\right)} \quad \beta = k_2/k_1 \tag{1}$$

The averaged stiffness coefficient and the natural frequency corresponding to the above period T are

$$T = \frac{4k_1k_2}{(\sqrt{k_1}+\sqrt{k_2})^2} \qquad \omega_n = \frac{2\pi}{T} = \sqrt{K/m} \tag{2}$$

The critical damping coefficient is obtained as

$$C_{cr} = 2\sqrt{Km} = 2m\omega_n \tag{3}$$

The governing second order ordinary differential equation (Chopra 1995, Clough and Penzien 1993) is stated as

$$m\ddot{y} + c_i\dot{y} + k_iy = F(t) \quad \text{where} \quad i = 1, 2 \tag{4}$$

Possible models of the above bilinear dynamical system include the following:

(1) Model-I

In this model, an equivalent mechanical system is envisaged with the single value of the stiffness K and damping coefficient C are obtained as

$$k_i = K \quad \text{and} \quad c_i = C = \xi C_{cr} \tag{5}$$

The governing differential equation turns out to be

$$m\ddot{y} + C\dot{y} + Ky = F(t) \tag{6}$$

(2) Model-II

This model, adopted by Thompson *et al.* (Thompson *et al*. 1983, Thompson *et al*. 1984, Thompson and Elvey 1984, Thompson and Stewart 1986) to simulate the dynamics of moored buoys, assigns the actual value k_1 or k_2 to the stiffness coefficient depending on the sense of the vibration amplitude but only one value C to the damping coefficient as per the above expression based on averaged stiffness. The resulting differential equation is stated as

$$m\ddot{y} + C\dot{y} + k_iy = F(t) \quad \text{where} \quad i = 1, 2 \tag{7}$$

This equation can be rewritten as

$$m\ddot{y} + 2\xi_i m\omega_{n_r}\dot{y} + k_iy = F(t) \quad \text{where} \quad i = 1, 2 \tag{8}$$

For the same value C of the damping coefficient, following two values of the damping ratios ξ_1 and ξ_2 are obtained for different sense of vibration amplitude.

$$\xi_1 C_{cr1} = \xi_2 C_{cr2} = C \quad \text{and} \quad C_{cri} = 2\sqrt{k_im} \quad \text{for} \quad i = 1, 2 \tag{9}$$

This model has been implemented for simulating the dynamical behavior of cracked concrete structures by the authors (Pandey and Benipal 2006, Pandey 2008).

(3) Model-III

As argued in the introduction, in this general bilinear model, two distinct values k_1 and k_2 are assigned to stiffness coefficient. The corresponding values c_1 and c_2 of the damping coefficient are obtained as follows

$$c_1 = 2\xi\sqrt{k_1m} \quad \text{and} \quad c_2 = 2\xi\sqrt{k_2m} \tag{10}$$

The Eq. (4) represents the relevant differential equation of motion for the model.

The bilinear system is considered to be under the action of a constant sustained load F_1 and a sinusoidal load with absolute peak magnitude F_2. Thus

$$F(t) = F_1 + F_2 \sin\omega_f t \tag{11}$$

So long as the sense of the vibration amplitude remains same, the bilinear system behaves as a conventional linear damped SDOF dynamical system and its motion is described by the well-known solution of the governing differential equation. The solution for Model-II is presented below. The same solution can be used for other models as well. For Model-I, ξ_1 and ξ_2 are assigned the same value ξ and ω_{n1} and ω_{n2} are assigned the same value ω_n. For Model-III, ξ_1 and ξ_2 are assigned the same value ξ.

The particular integral y_{Pi} and the complementary solution y_{ci} for the above first order linear differential equation are obtained as follows

$$y_{P_i} = \frac{F_1}{k_i} + \frac{F_2}{k_i}[P\sin\omega_f t + Q\cos\omega_f t] \tag{12}$$

$$y_{c_i} = e^{-\xi_i \omega_{n_i} t}(R\sin\omega_{D_i} t + S\cos\omega_{D_i} t) \tag{13}$$

where $\omega_{D_i} = \omega_{n_i}\sqrt{[1-\xi_i^2]}$, $\omega_{n_i} = \sqrt{\frac{k_i}{m}}$, and $\eta = \frac{\omega_f}{\omega_n}$

The general solution is obtained by superimposing the particular integral and the complimentary solution as

$$y = \frac{F_1}{k_i} + \frac{F_2}{k_i}[P\sin\omega_f t + Q\cos\omega_f t] + e^{-\xi_i \omega_{n_i} t}(R\sin\omega_{D_i} t + S\cos\omega_{D_i} t) \tag{14}$$

The constants P, Q, R and S are obtained from the initial conditions. As the vibration amplitude changes sign, the values of the stiffness coefficient and the damping coefficient, if applicable, undergo sudden change and the initial conditions for further motion also change. Each half cycle with positive or negative amplitude commences at initial or starting instant of time t_i and the corresponding initial conditions are stated as $y = y_s = 0$ and $\dot{y} = V_s$. The values of the parameters P, Q, R and S are obtained as

$$P = \frac{\left[1-\left(\frac{\omega_f}{\omega_{n_i}}\right)^2\right]}{\left\{\left[1-\left(\frac{\omega_f}{\omega_{n_i}}\right)^2\right]^2 + \left[-2\xi_i\frac{\omega_f}{\omega_{n_i}}\right]^2\right\}}$$

$$Q = \frac{\left[-2\xi_i\frac{\omega_f}{\omega_{n_i}}\right]}{\left\{\left[1-\left(\frac{\omega_f}{\omega_{n_i}}\right)^2\right]^2 + \left[-2\xi_i\frac{\omega_f}{\omega_{n_i}}\right]^2\right\}}$$

$$R = e^{\xi_i\omega_{n_i}t_i}\left[y_S - \frac{F_1}{k_i} - \frac{F_2}{k_i}\{P\sin\omega_f t_i + Q\cos\omega_f t_i\}\right]\sin\omega_{D_i}t_i +$$

$$\frac{e^{\xi_i\omega_{n_i}t_i}\cos\omega_{D_i}t_i}{\omega_{D_i}}\left[V_S + \xi_i\omega_{n_i}\left\{y_S - \frac{F_1}{k_i} - \frac{F_2}{k_i}(P\sin\omega_f t_i + Q\cos\omega_f t_i)\right\} - \frac{\omega_f F_2}{k_i}\{P\cos\omega_f t_i - Q\sin\omega_f t_i\}\right]$$

$$S = e^{\xi_i\omega_{n_i}t_i}\left[y_S - \frac{F_1}{k_i} - \frac{F_2}{k_i}\{P\sin\omega_f t_i + Q\cos\omega_f t_i\}\right]\cos\omega_{D_i}t_i -$$

$$\frac{e^{\xi_i\omega_{n_i}t_i}\sin\omega_{D_i}t_i}{\omega_{D_i}}\left[V_S + \xi_i\omega_{n_i}\left\{y_S - \frac{F_1}{k_i} - \frac{F_2}{k_i}(P\sin\omega_f t_i + Q\cos\omega_f t_i)\right\} - \frac{\omega_f F_2}{k_i}\{P\cos\omega_f t_i - Q\sin\omega_f t_i\}\right] \quad (15)$$

Similarly, the expressions for velocity and acceleration are obtained as

$$\dot{y} = \frac{F_2\omega_f}{k_i}[P\cos\omega_f t - Q\sin\omega_f t] + e^{-\xi_i\omega_{n_i}t}\omega_{D_i}(R\cos\omega_{D_i}t - S\sin\omega_{D_i}t)$$
$$- e^{-\xi_i\omega_{n_i}t}\xi\omega_{n_i}(R\sin\omega_{D_i}t + S\cos\omega_{D_i}t) \quad (16)$$

$$\ddot{y} = \frac{-F_2\omega_f^2}{k_i}[P\sin\omega_f t + Q\cos\omega_f t] - e^{-\xi_i\omega_{n_i}t}\omega_{D_i}^2(R\sin\omega_{D_i}t + S\cos\omega_{D_i}t)$$
$$- e^{-\xi_i\omega_{n_i}t}\xi_i\omega_{n_i}\omega_{D_i}(R\cos\omega_{D_i}t - S\sin\omega_{D_i}t)$$
$$- e^{-\xi_i\omega_{n_i}t}\xi_i\omega_{n_i}\omega_{D_i}(R\cos\omega_{D_i}t - S\sin\omega_{D_i}t) + e^{-\xi_i\omega_{n_i}t}(\xi_i\omega_{n_i})^2(R\sin\omega_{D_i}t + S\cos\omega_{D_i}t) \quad (17)$$

Also, the inertial force, damping force, elastic force and total force are defined as

$$F_{In} = m\ddot{y}; \quad F_D = c_i\dot{y}; \quad F_E = k_i y; \quad F_T = F_{In} + F_D + F_E \quad (18)$$

3. Numerical computations

The chosen object of study in this paper is a massless simply supported reinforced concrete beam with a lumped mass located at mid span and subjected to vertical constant and sinusoidal forces. The computed dynamical response of this SDOF system pertains to the following numerical details of the beam:

Span (L) = 8 m, width (b) = 200 mm, gross depth (D) = 400 mm, steel cover = 40 mm
Materials: M50 grade concrete and Fe 415 grade steel,
Modulus of elasticity of concrete, $E_c = 5000\ (f_{ck})^{1/2}$
Lumped mass at the centre (m) = 800 kg, Damping ratio (ξ) = 0.05
Stiffness: k_1 = 311018.7 N/m, k_2 = 2488149.6 N/m, β = 8, K = 679040.55N/m, K_{gross}= 3535533.9 N/m
Natural frequencies: ω_n = 29.134184 rad/s, ω_{n1} = 19.717331 rad/s, ω_{n2} = 55.769050 rad/s

Damped frequency (Averaged): $\omega_D = 29.0977434379$ rad/s
Natural periods: $T = 0.2156636$ s, $T_1 = 0.3186629$ s, $T_2 = 0.1126643$ s, $T_D = 0.2156933$ s
Damping coefficients: $C = 2330.7347$ N-s/m, $c_1 = 1577.3869$ N-s/m, $c_2 = 4461.5240$ N-s/m

Unless otherwise stated, the peak sinusoidal force F_2 has been assumed to be ±20 kN. The magnitude of the constant sustained load F_1 has been varied as a multiple of the peak sinusoidal force. The constant and sinusoidal forces acting vertically downwards and the corresponding displacements and vibration amplitudes have been taken as negative.

4. Discussion of the results computed

In this paper, the dynamic response of Model-I and Model-III of the above bilinear dynamical system to sinusoidal loading has been predicted. For clarity of presentation, it is necessary to distinguish among the three different linear systems investigated. In this paper, of course, Model-I of the bilinear system is one of these linear systems and has stiffness equal to average stiffness K of the cracked reinforced concrete structures modeled as a bilinear system. In contrast, the approximate linear model employed by structural designers for static and dynamic analysis presumes stiffness K_{gross} of the uncracked unreinforced beam section (IS-1893 2002, IS-456 2000). Also, for the special case of bilinearity ratio of unity, the Model-III also reduces to a linear system but with stiffness equal to k_1. As all of these linear systems have same damping ratio of five percent, the different values of their stiffness coefficients result in different value of their damping coefficients as well.

The waveforms for the displacement, velocity and acceleration response as well as phase plots (also called Poincare diagrams) for Model-I, Model-II and Model-III of the same bilinear oscillator executing free vibrations with identical initial conditions ($y_0 = -0.25$ m, $V_0 = 0$ m/s) have been shown in Fig. 1. As expected from linear oscillators, Model-I exhibits sinusoidal wave forms and an elliptical phase plot. In contrast to Model-I, the remaining models exhibit different peak positive and negative magnitudes of amplitude, velocity and acceleration. However, such an effect is not much for velocity response. During the excursions of the mass towards positive and negative displacements respectively, the vibrations are sinusoidal with a discontinuity as and when the vibration amplitude is zero. The phase plots for Model-II and Model-III can be observed to be composed of two half ellipses. Like all damped systems, the vibrations are damped out asymptotically. It has been verified for Model-II and Model-III from their waveforms for natural vibrations that the natural period of the system is independent of the initial perturbations. This finding implies that, in this respect, these bilinear systems resemble conventional linear dynamical systems.

The above observations are confirmed by frequency domain response curves presented earlier (Pandey and Benipal 2006) for Model-II and in Fig. 2 in this paper for Model-III. In these forced vibrations, the magnitude of the peak sinusoidal force has been kept equal to 20 kN. Even though, both the positive and negative resonance response curves exhibit multiple resonance peaks at the same frequency ratios, the steady state response can be seen to be richer in detail than the absolute maximum response. It can be observed that the positive peak amplitudes exceed the negative peak amplitudes at all frequency ratios for both the steady state and absolute responses.

Apart from the fundamental response, the regular sub-harmonic resonance peaks are observed

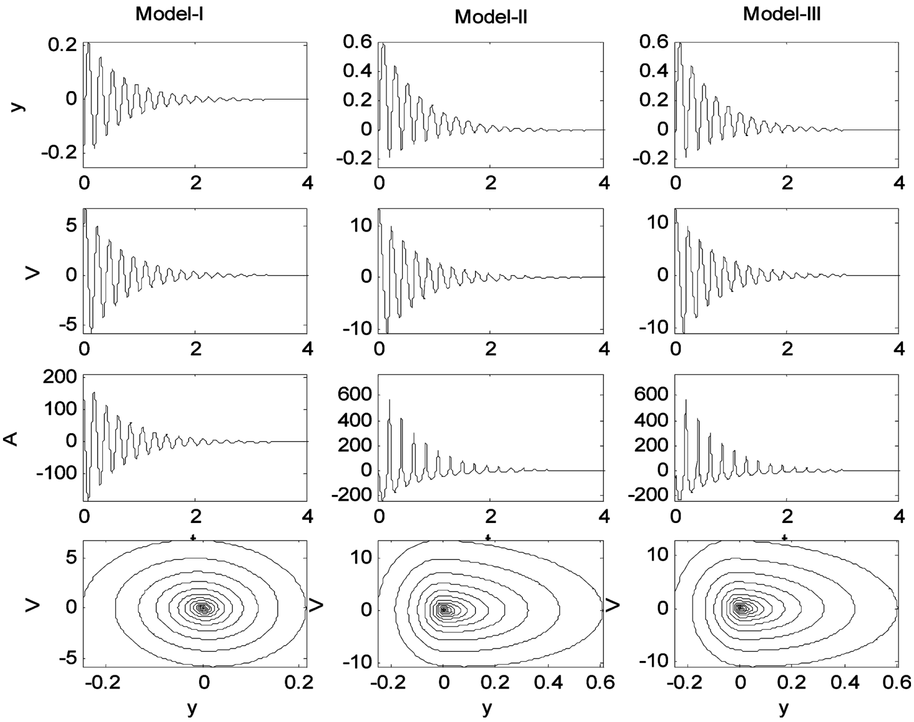

Fig. 1 Free vibration displacement, velocity, acceleration response and phase plots for different models

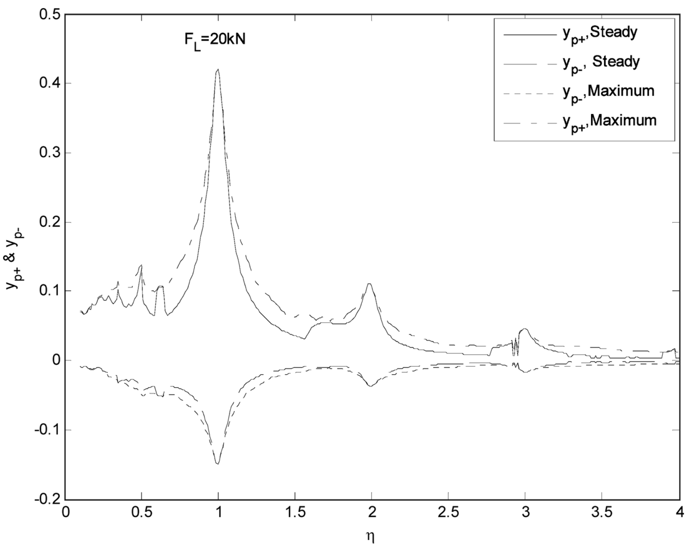

Fig. 2 Peak positive and peak negative responses and corresponding steady state responses for Model-III

approximately at frequency ratios 1.99, 2.99, 3.99, etc., as well as the irregular sub-harmonics at frequency ratios 0.5, 0.35, 0.10, etc. In these respects, the Model-II and Model-III predictions are qualitatively similar. Like Model-II, it has been verified, though not presented here, that the sub-

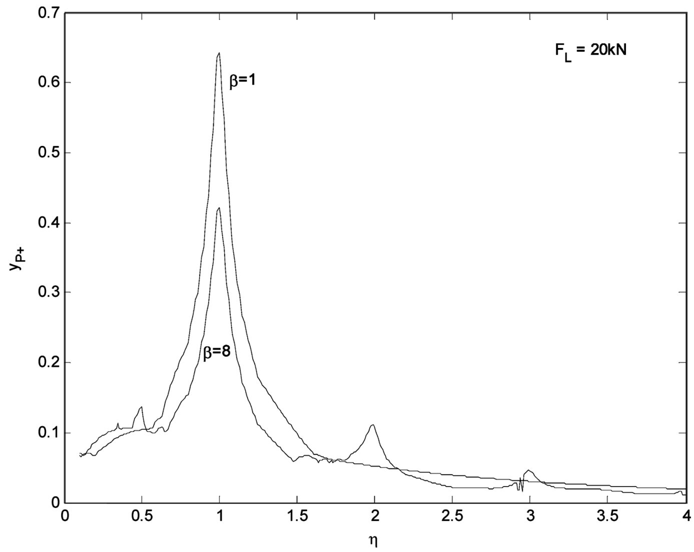

Fig. 3 Resonance response curve for Model-III (F_2 = 20 kN, β = 1 and 8, ξ = 0.05)

harmonic resonance peaks become more prominent whereas the fundamental resonance peak response becomes less prominent at higher values of bilinearity ratio. This is because of the fact that these curves are plotted by keeping the lower stiffness k_1 constant and by increasing the higher stiffness k_2 to obtain higher values of bilinearity ratio. This results in the systems with higher bilinearity ratio being stiffer showing lower fundamental peak response. However, effect of bilinearity ratio on sub-harmonic peaks can not be explained by this argument. Some of the most distinguishing characteristics of the bilinear dynamical systems can be identified from Fig. 3 showing peak positive resonance response curves for Model-III for the two values of bilinearity ratio. The resonance response curve for linear dynamical system with bilinearity ratio of unity exhibits the expected smooth resonance response with single peak at its natural frequency. In contrast, the frequency domain response of other system with bilinearity ratio of eight is distinguished by regular as well as irregular sub-harmonics. Still, in both of these systems, the system response asymptotically vanishes as the bilinearity ratio increases. As expected, the fundamental peak response of stiffer system with higher bilinearity ratio is found to be lower. However, the sub-harmonic peaks of the latter system (β = 8) imply higher peak amplitudes than the system (β = 1) at the corresponding frequency ratios.

The linear system response gradually diminishes with increase in frequency ratio. In the case of conventional unilinear systems, the peak amplitudes are useful for ensuring the serviceability as well as the safety of the structures under dynamic forces. This is so because of the fact that the peak elastic forces responsible for causing structural failure are proportional to the peak amplitudes. Such is not the case for bilinear systems which exhibit different positive and negative peak amplitudes and have different corresponding stiffness coefficients. The absolute value of the peak amplitude is expected to govern the serviceability criterion. Also, for these systems, the higher peak amplitudes correspond to lower stiffness and so do not imply higher peak elastic forces. The variation of the positive as well as negative peak elastic forces with frequency ratio has been plotted in Fig. 4. It can be observed that the negative peak elastic forces are higher at all frequency ratios, even though

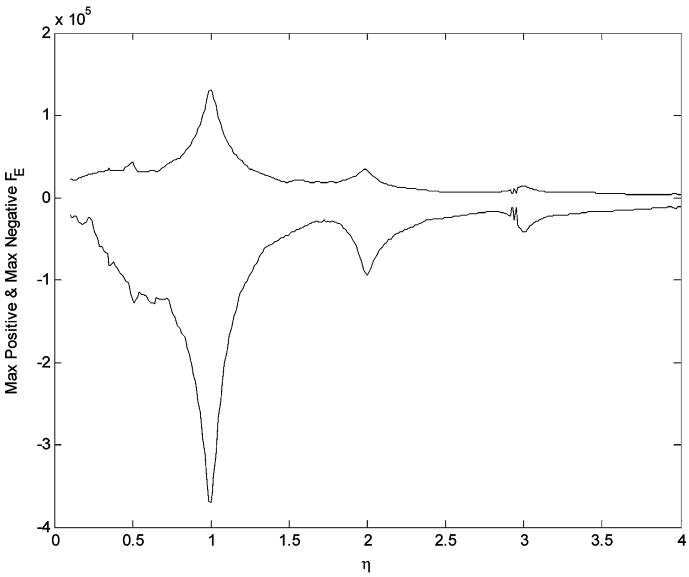

Fig. 4 Maximum positive and negative elastic forces vs η (F_2 = 20 kN, β = 8, ξ = 0.05)

the corresponding peak amplitudes are lower. However, it can not be concluded that the higher peak elastic forces determine the structural safety margins because the strength also depends upon the sense of the amplitude. For example, the ultimate flexural moment of resistance for a reinforced concrete beam is higher for the sense of the moments corresponding to higher stiffness. Also, the presence of sub-harmonic peak elastic forces has significant implications for structural design.

The frequency domain analysis of equivalent unilinear Model-I is presented and compared with bilinear Model-III and with the approximate unilinear analysis based on gross stiffness K_{gross}. As expected from the unilinear systems, the sub-harmonic resonance peaks are absent for Model-I in the relevant curve shown in Fig. 5. This constitutes a shortcoming of this equivalent unilinear model of the actual bilinear dynamical system exhibiting sub-harmonics. Also, as an essentially linear system, Model-I is expected to exhibit the same positive and negative fundamental peak response. The magnitude of the peak fundamental response for Model-I is obtained to be lesser than that for the positive peak fundamental response but higher than the negative peak fundamental response of Model-III. It has been verified for the present case that the stiffness K_{gross} of the uncracked unreinforced concrete section generally exceeds the averaged value of stiffness K of Model-I. Obviously, the approximate method of dynamic analysis based upon gross stiffness predicts lower system response at all frequency ratios.

The above frequency domain analysis has been conducted by varying the frequency ratio achieved by varying forcing frequency but keeping the natural frequency of the system constant. It implies that the response of the same dynamical system subjected to different forcing frequencies has been investigated. In the next Fig. 6, the response of dynamical systems with different natural frequencies or time periods subjected to same forcing frequency (ω_f = 6 rad/s) is presented. The absolute positive and negative peak responses of both the Model-III and Model-I of the chosen bilinear system have been compared. The bilinear dynamical systems with bilinearity ratio of eight but with different natural periods refer to systems with different values of lower stiffness k_1. The peak

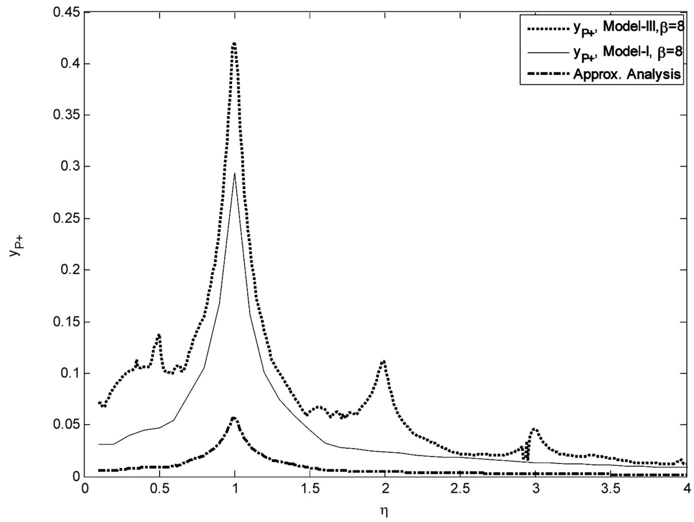

Fig. 5 Resonance responses with frequency ratio of the system

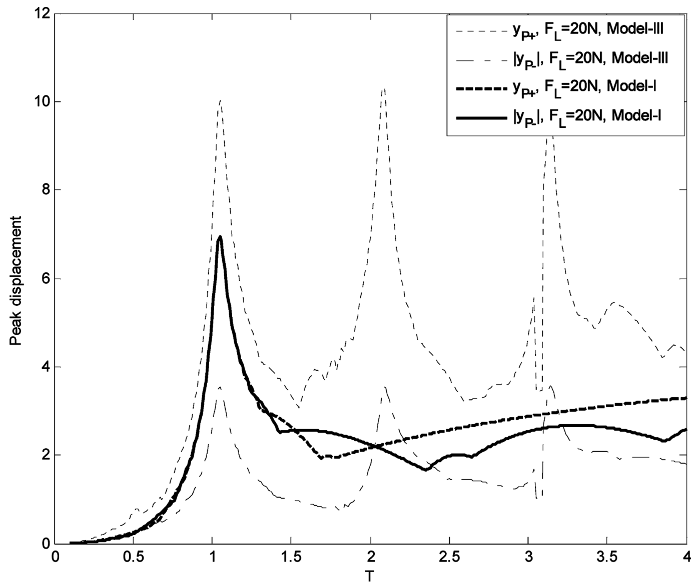

Fig. 6 Peak positive and absolute value of peak negative response with natural period T for Model-I and Model-III

amplitudes plotted in this figure pertain to the higher (positive) amplitude on the side of lower stiffness k_1. Thus, the systems with longer periods are more flexible and so exhibit higher positive peak response. This observation is confirmed by the magnified values of regular sub-harmonics at periods 2.1 s and 3.15 s respectively. So much so, these sub-harmonic peak amplitudes are of approximately the same order as the fundamental response occurring at fundamental period 1.05 s. In contrast, for the same reason, the irregular sub-harmonic peaks are suppressed. The fundamental time period of 1.05 s corresponds to the chosen forcing frequency of 6 rad/s. As expected, the negative peak amplitudes corresponding to higher stiffness k_2 turn out to be of smaller magnitude. Model-I, being linear, does not exhibit sub-harmonics, but only the fundamental peak response. Also, in line with the conclusion drawn earlier, the response computed using Model-I, in general, lies between the absolute positive and negative peak responses with the exception that the sub-harmonic peaks at 2.1 s and 3.15 s exceed the Model-I response. Since the unilinear structures with longer periods also become more flexible, the system response increases at longer periods. It should be noted that it is the absolute peak response, not the steady peak response, which has been plotted in that figure. As its absolute peak response is affected by the transients, even the linear system (Model-I) exhibits different positive and negative peak responses.

When compared with the approximate method based upon the stiffness of the gross uncracked unreinforced section, the equivalent unilinear model turns out to be a more realistic model. As per the current design practice recommended in seismic codes (IS-1893 2002), the natural time period of the structural system is based on the stiffness of gross section. However, it is a known fact that the concrete structures are cracked at working loads and it should be more relevant to take the natural time period based on the cracked section stiffness. The period calculated for the cracked section depends upon the percentage of top and bottom reinforcement as well as on the grade of concrete. In Fig. 7, the variation of the period with bottom (tension) steel for different percentages of top (compression) steel has been plotted for M50 grade of concrete. The natural periods have been determined by using the averaged stiffness K of Model-I. The periods for the chosen particular beam vary from 0.0917 s to 0.327 s for the cracked section in contrast to the constant period of 0.0945 s calculated from gross section. It can be concluded that, for the common amounts of tension and compression reinforcement, the period of cracked beams can be 2-3 times more than that estimated for the gross section.

As stated above, the averaged stiffness K of Model-I is generally lower that that of the gross section. Also, their damping ratios being equal, the damping coefficient implied in Model-I is lower than that for the approximate method. It should be noted that the linear systems with the same

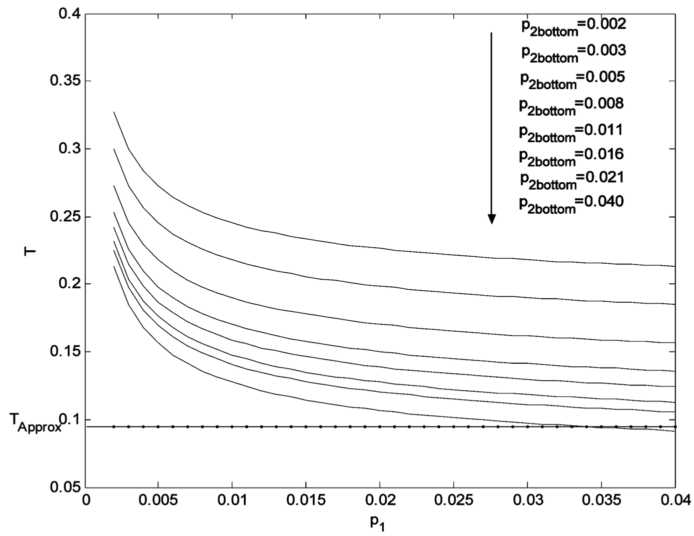

Fig. 7 Variation of averaged natural period of the beam for different top and bottom reinforcement

period have the same corresponding stiffness, the vibrating mass being constant. In view of this fact, the curve in Fig. 6 for Model-I also represents the approximate method. For the reinforced concrete beam with details given above, the Model-I and the approximate method have relevant stiffness values of K and K_{gross} respectively, the corresponding natural periods being 0.2156 s and 0.0945 s. Naturally, the response of two linear systems with different periods is expected to be different. As can be seen from Fig. 5, the Model-I and the approximate method predict different responses of the system subjected to the same forcing frequency. The actual difference in their predictions is expected to depend on the absolute values of their time periods, depending upon the top and bottom reinforcement as shown in Fig. 7, of the assumed mechanical systems.

In the following computational studies on forced vibrations, the peak magnitude of the sinusoidal force F_2 has been kept equal to −20 kN. Also, the initial displacement and velocity refer to the passive state (y = 0 m, V = 0 m/s). After various trials, it has been found that the system with bilinear stiffness and bilinear damping exhibits resonance response of various orders (n = 1, 2, 3 and 4) approximately at frequency ratios 1, 1.99, 2.99 and 3.99 respectively. The response waveforms for resonant responses of different orders have been determined and presented graphically in Fig. 8 to Fig. 13. The conclusions concerning the relative magnitudes of the steady state peak positive and negative vibration excursions are confirmed here. Also, the response frequency of the fundamental response turns out to be equal to the forcing frequency, whereas the response frequencies of the resonance responses of order 2, 3 and 4 are obtained as one-half, one-third and one-fourth of its value. The resonant waveforms for the irregular sub-harmonics have been

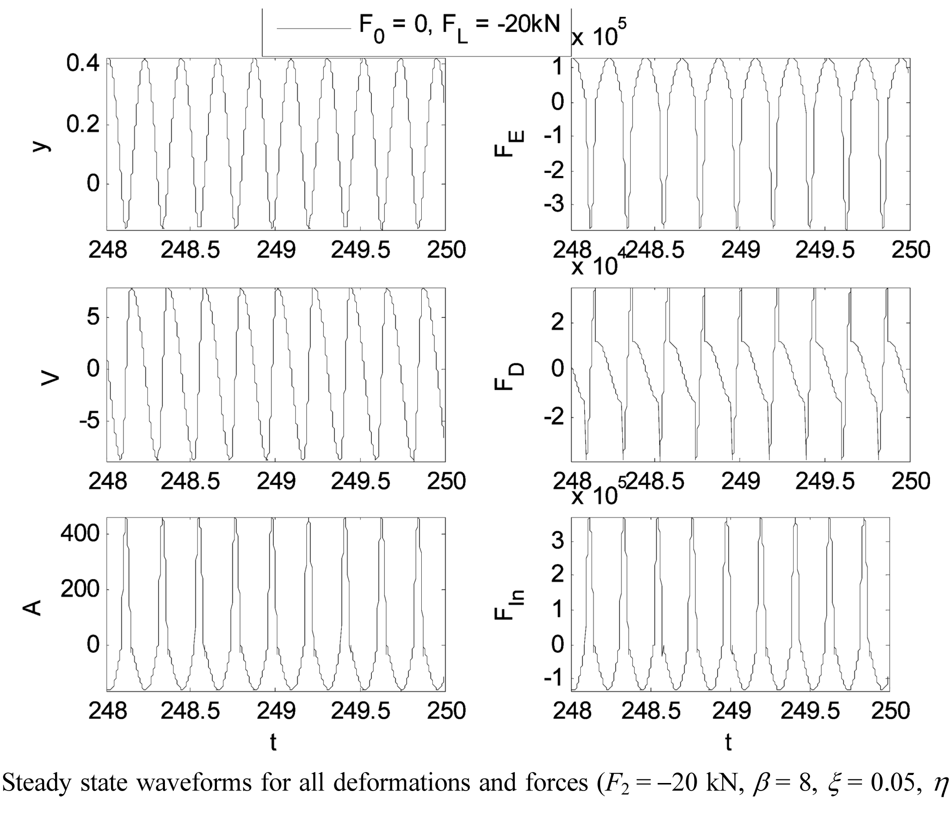

Fig. 8 Steady state waveforms for all deformations and forces (F_2 = −20 kN, β = 8, ξ = 0.05, η = 1.0)

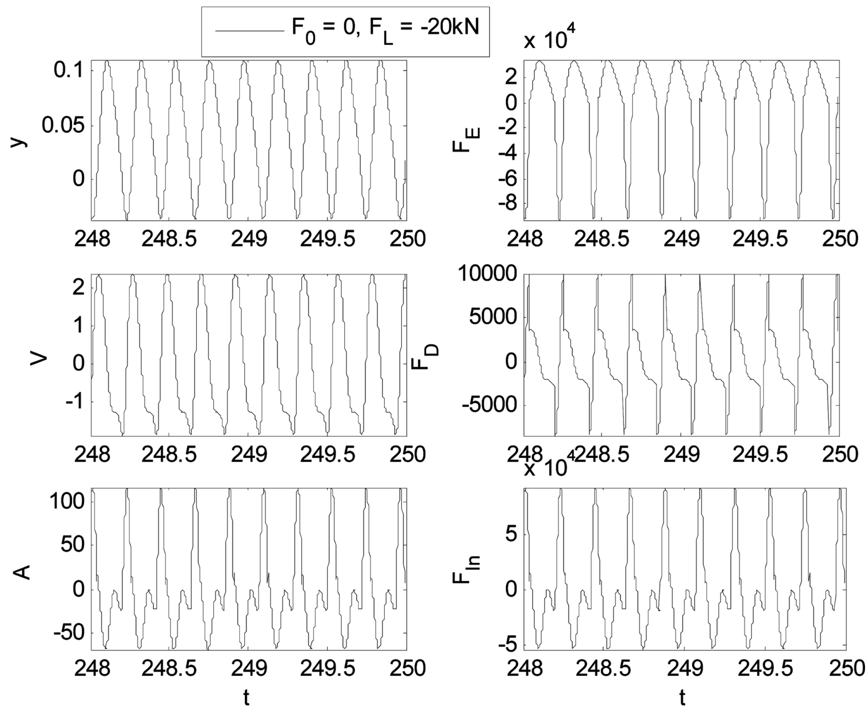

Fig. 9 Steady state waveforms for all deformations and forces ($F_2 = -20$ kN, $\beta = 8$, $\xi = 0.05$, $\eta = 1.99$)

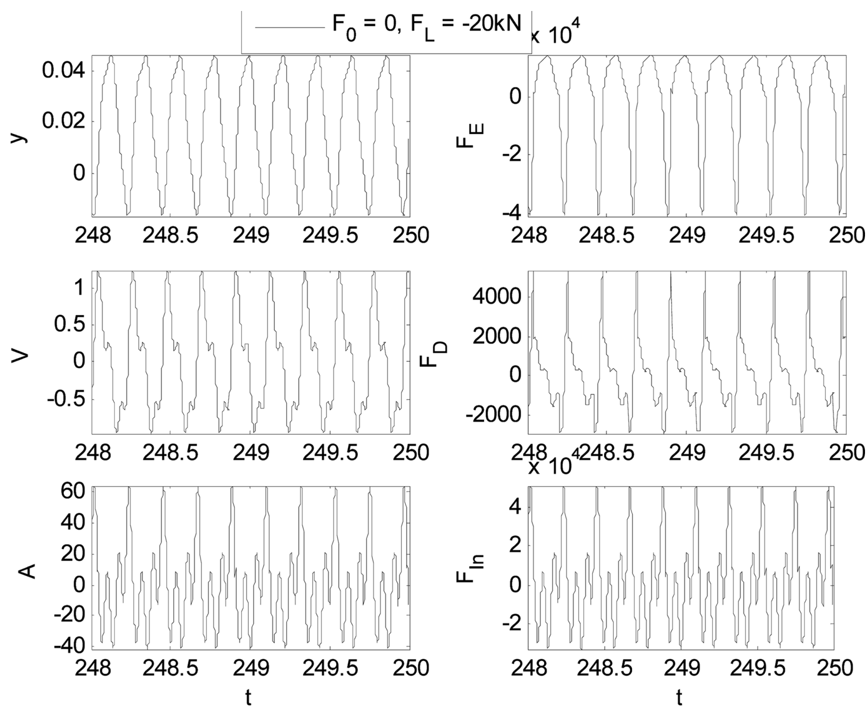

Fig. 10 Steady state waveforms for all deformations and forces ($F_2 = -20$ kN, $\beta = 8$, $\xi = 0.05$, $\eta = 2.99$)

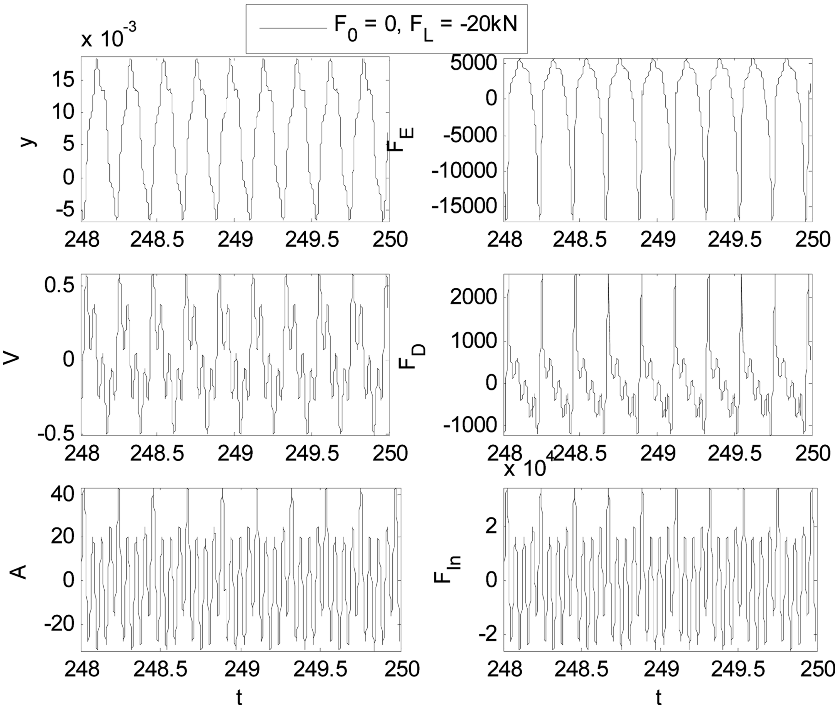

Fig. 11 Steady state waveforms for all deformations and forces ($F_2 = -20$ kN, $\beta = 8$, $\xi = 0.05$, $\eta = 3.99$)

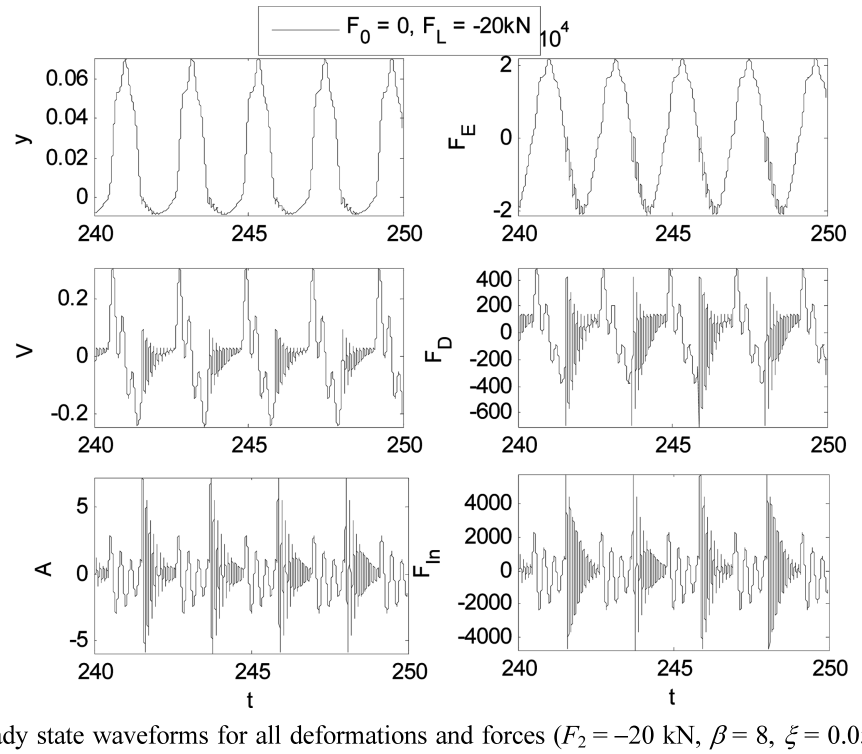

Fig. 12 Steady state waveforms for all deformations and forces ($F_2 = -20$ kN, $\beta = 8$, $\xi = 0.05$, $\eta = 0.10$)

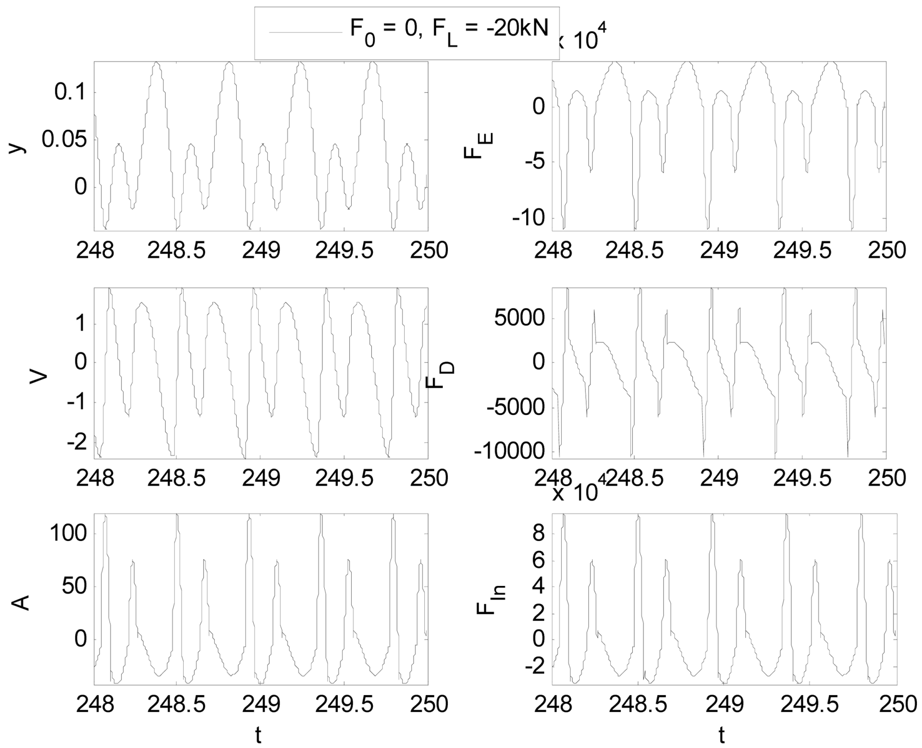

Fig. 13 Steady state waveforms for all deformations and forces ($F_2 = -20$ kN, $\beta = 8$, $\xi = 0.05$, $\eta = 0.50$)

plotted for frequency ratios 0.1 and 0.5. In these waveforms, one relatively large excursion into the low stiffness domain is succeeded by an integral number of small oscillations which vanish gradually. It must be remembered, however, that these irregular sub-harmonic resonances are always assigned order unity.

In the above figures, the steady state waveforms for elastic, damping and inertial forces have also been shown to follow the corresponding waveform for displacement, velocity and acceleration respectively with some modification. These forces depend upon the operative stiffness coefficient, damping coefficient and mass apart from the displacement, velocity and acceleration of the system. For example, the negative peak elastic force turns out to be higher in spite of the fact that negative peak displacement is lower. Likewise, the positive peak values of velocity, acceleration, damping force and inertial force are different from the corresponding negative peak values for vibrations of various orders. The effect of sudden change in damping coefficient with change in sense of vibration amplitude is investigated later.

Corresponding to each waveform of the resonant response, the phase plots have also been presented in Fig. 14. It can be observed that the phase plot for the fundamental response is composed of two half ellipses of different lengths of major and minor axes. In contrast, more complicated phase plots are obtained for higher order resonance responses. For example, while the third and fourth order phase plots respectively exhibit one and three crossover points, the trajectories in the second order response, like the fundamental one, lack such crossover points. The phase plots for the irregular sub-harmonic resonances confirm the presence of one large excursion

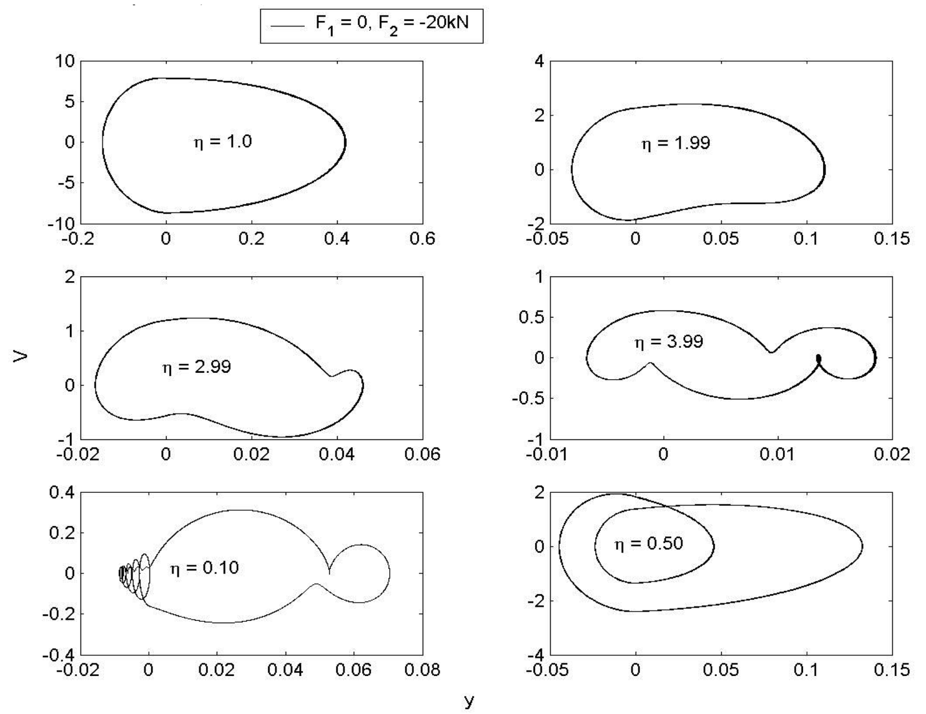

Fig. 14 Phase plot representation for response of different orders ($F_2 = -20$ kN, $\beta = 8$, $\xi = 0.05$)

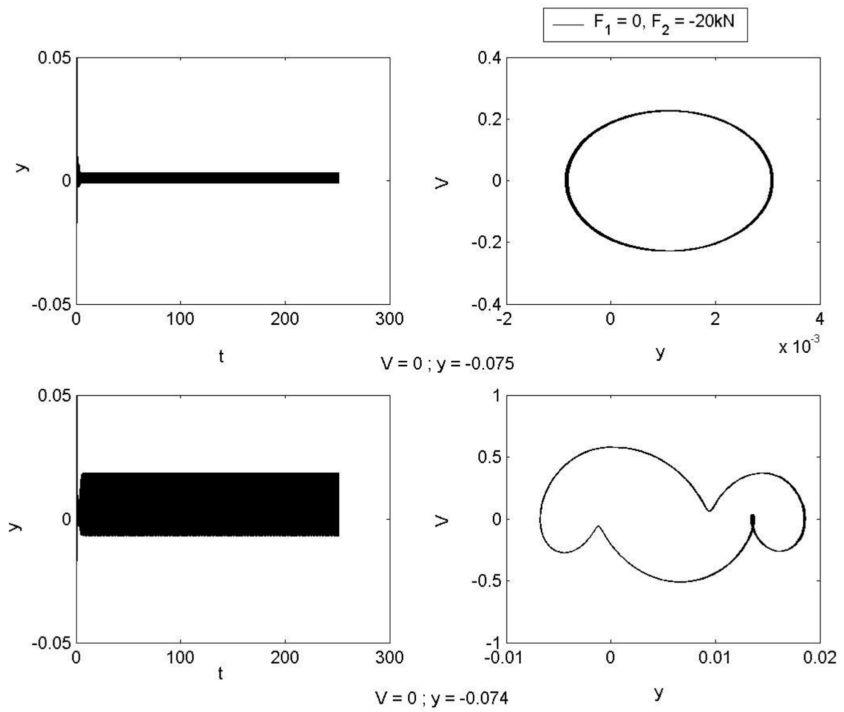

Fig. 15 Sensitivity to initial conditions ($F_2 = -20$ kN, $\beta = 8$, $\xi = 0.05$, $\eta = 3.99$)

succeeded by a number of small amplitude damped vibrations. The above waveforms and phase plots for steady state oscillations of various orders for Model-III resemble those for Model-II investigated earlier (Pandey and Benipal 2006).

Like other nonlinear systems, the bilinear mechanical system investigated in this paper also exhibits strong sensitivity to initial conditions. As shown in Fig. 15, two identical bilinear dynamical systems (Model-III) under the action of identical forcing functions (F_2 = –20 kN, η = 3.99) but with slightly different initial conditions (y = –0.075 m, V = 0 m/s) and (y = –0.074 m, V = 0 m/s) experience steady state vibrations with different peak amplitudes as shown in their waveforms. The corresponding phase plots reveal that their resonance responses are of order one and four respectively. It can be observed that the waveforms from adjacent starts diverge with time to such an extant that the corresponding steady state responses lack any correlation. Such nonunique behavior is exhibited for an infinitely large number of, but not all, pairs of adjacent starts in the phase plane. The system behavior with adjacent initial conditions gets settled into different steady state responses, called attractors, of order either one or four depending upon the particular initial conditions. The phase plane is thus divided into two distinct catchment regions or domains of attraction for these coexisting steady state periodic attractors. Since the system exhibits instability at the boundaries of the adjacent catchment regions, such a divided phase plane is called stability portrait in the space of initial conditions. Detailed computations have been performed for obtaining such stability portrait, shown in Fig. 16, of the present dynamical system. Such divergent systems are expected to exhibit instability in the dependence of their response on the system parameters like forcing frequency, time period, damping ratio, bilinearity ratio, etc., but such stability portrait in the parameter space has not been attempted here. However, the discontinuous effect of forcing frequency and time period of the system on dynamic response has been investigated below.

In the Fig. 8, the waveforms showing the temporal variation of displacement, velocity, acceleration as well as elastic, damping and inertial forces have been plotted for a particular case of

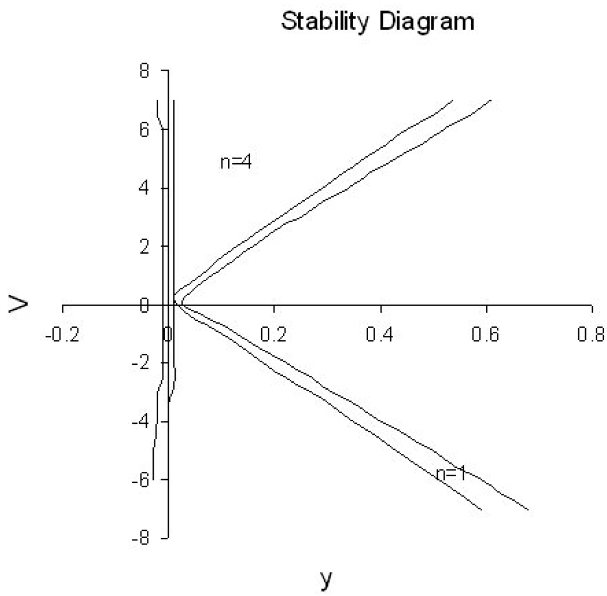

Fig. 16 Catchment regions for two periodic attractors (F_2 = 20 kN, β = 8, ξ = 0.05, η = 3.99)

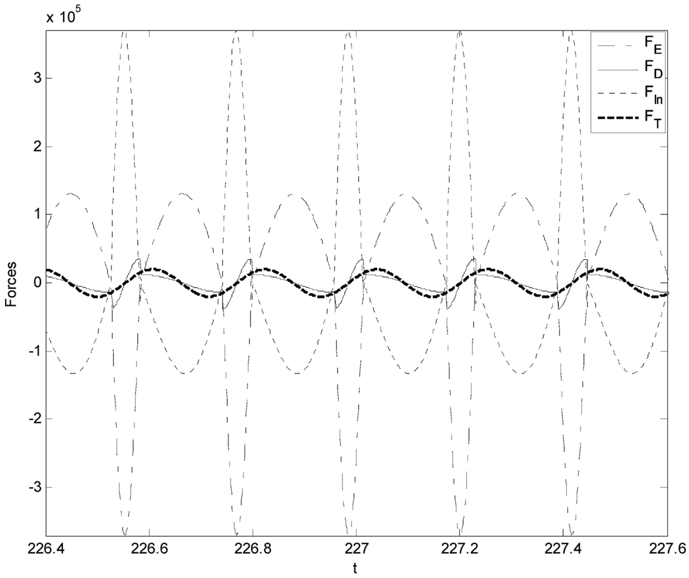

Fig. 17(a) Jump phenomena in damping and inertial forces ($\beta = 8$, $\eta = 1.0$ and $\xi = 0.05$)

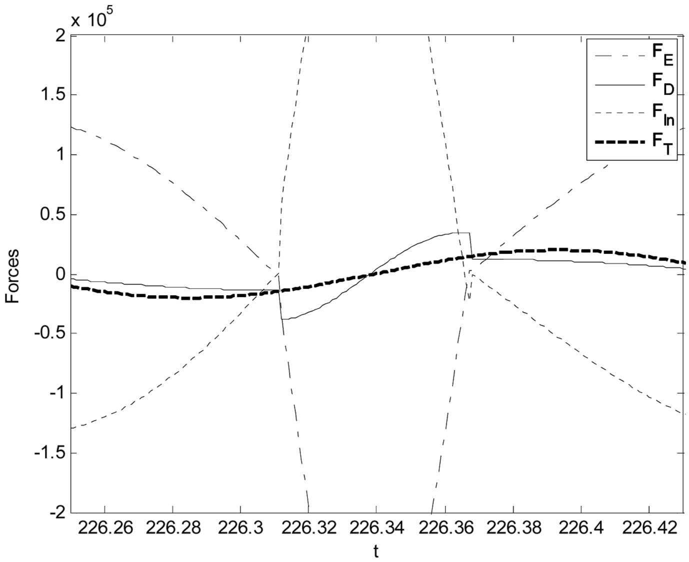

Fig. 17(b) Enlarged view of jump phenomena in damping and inertial forces ($\beta = 8$, $\eta = 1.0$ and $\xi = 0.05$)

frequency ratio of unity. The variation of displacement, velocity and elastic force is observed to be smooth whereas the waveforms for damping force, inertial force and acceleration exhibit jump phenomena in the form of sudden changes. This fact is depicted in Fig. 17(a) in which the steady state variation of elastic, damping, inertial and total applied forces has been superimposed. These jump phenomena are attributed to the fact that the value of the damping coefficient changes suddenly as and when the displacement experiences change in sense. This happens at the peak velocities resulting in a sudden change in the damping force. The applied force being sinusoidal, the sudden change in damping force introduces a corresponding sudden change of opposite sense in the inertial force. Since the mass remains invariant during vibrations, the waveform for acceleration also exhibits jump phenomenon at the same instant. A blow-up of the jump phenomena in the damping and inertial forces is presented in Fig. 17(b) for more clarity. It can be observed that, as the vibration amplitude changes sense from positive to negative, the damping coefficient experiences sudden change from the lower value c_1 to higher value c_2. Because of this fact, the damping force experiences a sudden increase in its magnitude whereas the inertial force makes up for it by experiencing a sudden decrease. The effect is of opposite nature when the vibration amplitude changes sense from negative to positive. The relative magnitudes of the various forces are also displayed. That the elastic and inertial forces are dominant in this particular case can be easily appreciated from this figure.

It has been verified that all resonance peak amplitudes including the fundamental as well as sub-harmonic resonances decrease with increase in damping ratio. At sufficiently high damping ratios, the sub-harmonics may even vanish. However, for the present bilinear system, the higher value of damping ratio accentuates the jump phenomena. As shown in Fig. 18, the sudden change in the damping force constitutes a substantial fraction of the total damping force at damping ratio of 0.2. In contrast, as shown in Fig. 17(a), the relative magnitude of the sudden change in damping force is considerably smaller for damping ratio of 0.05.

In general, the frequency and time domain behavior as well as phase planes for the dynamical system with bilinear stiffness and bilinear damping presented above are qualitatively similar to those for the dynamical system with constant damping investigated earlier by the authors (Pandey and Benipal 2006). However, the present system does not exhibit simultaneous overdamping/underdamping in the same vibration cycle. The distinguishing characteristic of the dynamical system studied here is the above jump phenomena in its response.

In addition, like other nonlinear dynamical systems, the bilinear dynamical systems exhibit

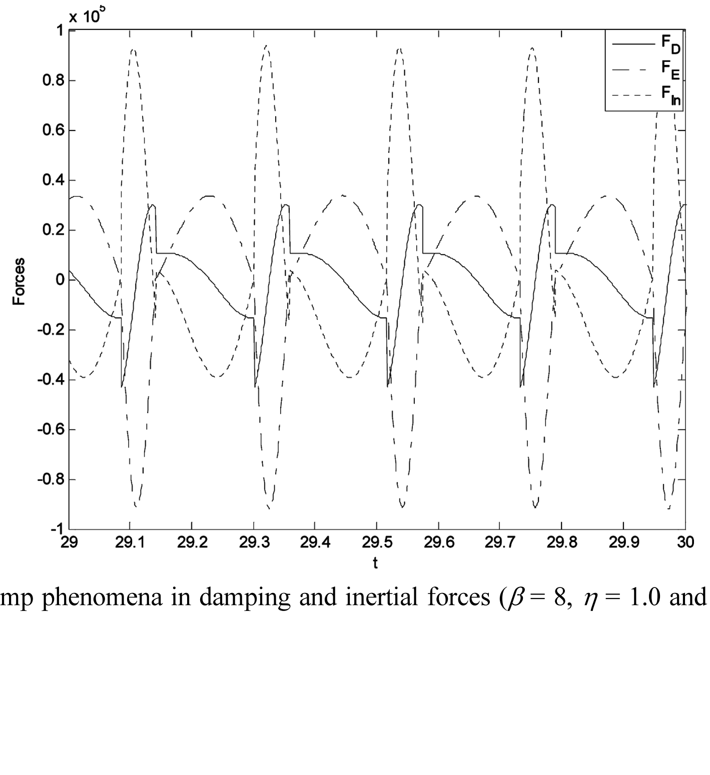

Fig. 18 Jump phenomena in damping and inertial forces ($\beta = 8$, $\eta = 1.0$ and $\xi = 0.20$)

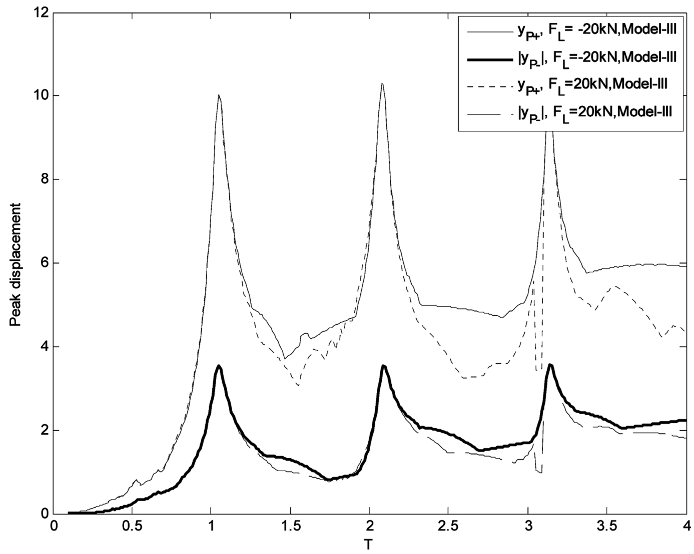

Fig. 19(a) Peak positive and absolute value of peak negative response spectra of Model-III for change of sense of forces

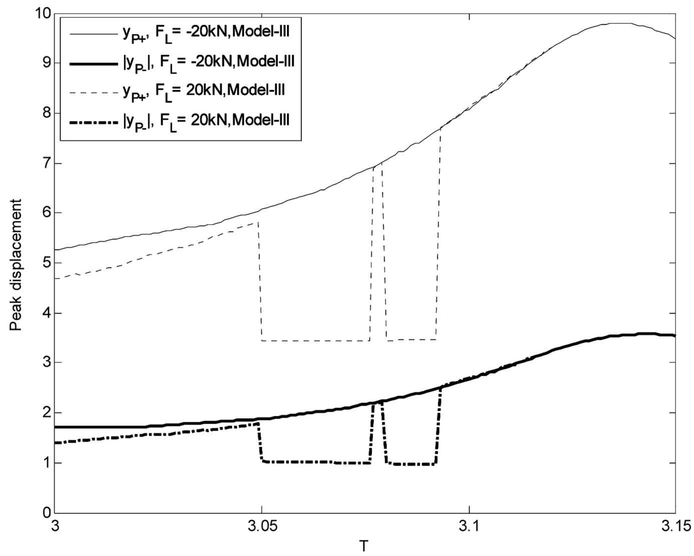

Fig. 19(b) Enlarged view of peak positive and absolute value of peak negative response spectra ofModel-III for change of sense of forces

discontinuities in the functional dependence of their response upon the initial conditions, system parameters and loading details. This observation is confirmed by the predicted variation of displacement response with frequency ratio and natural period as shown in Fig. 5 and Fig. 6 respectively. Strong discontinuities in system response are observed in the range 2.9-3.0 rad/s of the frequency ratio and in the range 3.0 s-3.1 s of the natural period. Such an interesting aspect of dynamical behavior of cracked concrete structures under service loads is discussed below:

The above response has been computed for the system under the action of peak sinusoidal force of 20 kN. It has been verified that the discontinuities in the system response vanish if the sense of the peak sinusoidal force is reversed. This fact is demonstrated in Fig. 19(a) showing the variation, with time period, of positive and negative absolute peak responses for Model-III under the action of positive as well as negative peak sinusoidal force. As in the case of frequency domain plot, the positive and negative absolute peak responses exhibit the similar trend. Also, it turns out that the system response to positive and negative peak sinusoidal forces coincides wherever the resonance peaks occur but differs considerably elsewhere. A blown up image of the discontinuities in the above figure has also been presented in Fig. 19(b). It can be observed that the system response is considerably richer in detail showing more discontinuities when observed at finer intervals of natural time periods. Except the discontinuities, the system response to positive and negative peak sinusoidal forces is similar. It can be observed from Fig. 19(b) that the peak amplitude responses for systems with natural periods slightly lesser than 3.051 s, between 3.077 s and 3.080 s, and periods slightly exceeding 3.092 s do not differ much from each other. However, the system response turns out to be much lower if the natural period of the system falls within the ranges 3.051 s-3.077 s or 3.080 s-3.092 s.

The steady state waveforms for the displacement and the elastic force as well as the phase plots for the two structures with periods equal to 3.05 s and 3.06 s respectively and subjected to positive peak sinusoidal force have been shown in Fig. 20. The observations made above concerning displacement response are confirmed in this figure. Also, the peak elastic forces for the system with slightly lower natural period turn out to be considerably higher. The phase plots for these two

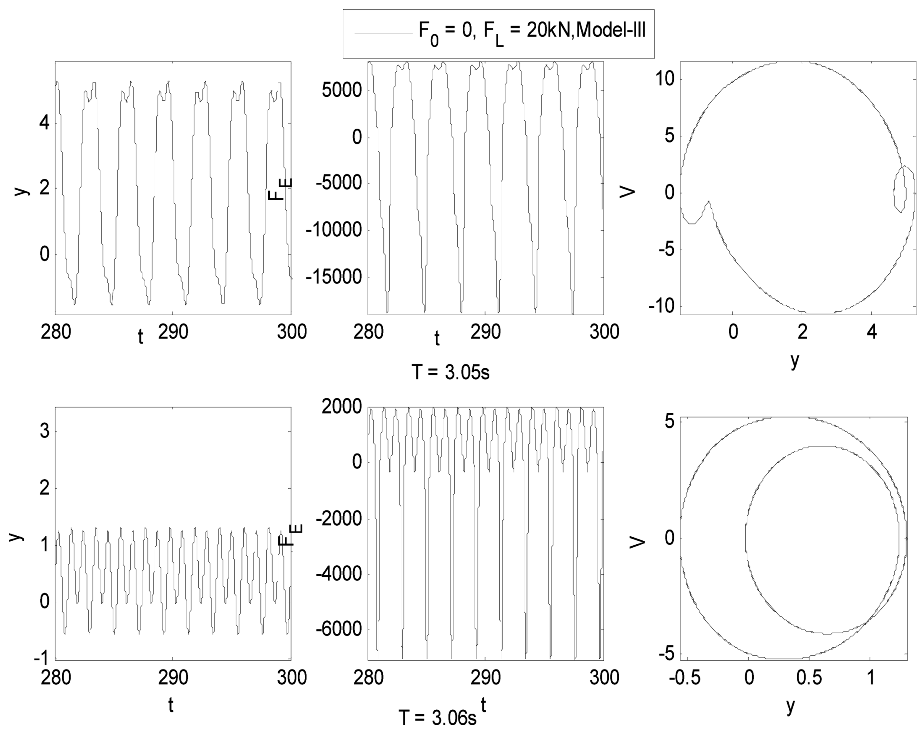

Fig. 20 Steady state waveforms of displacement and elastic force, and phase plot (F_2 = 20 kN, T = 3.05 s and T = 3.06 s)

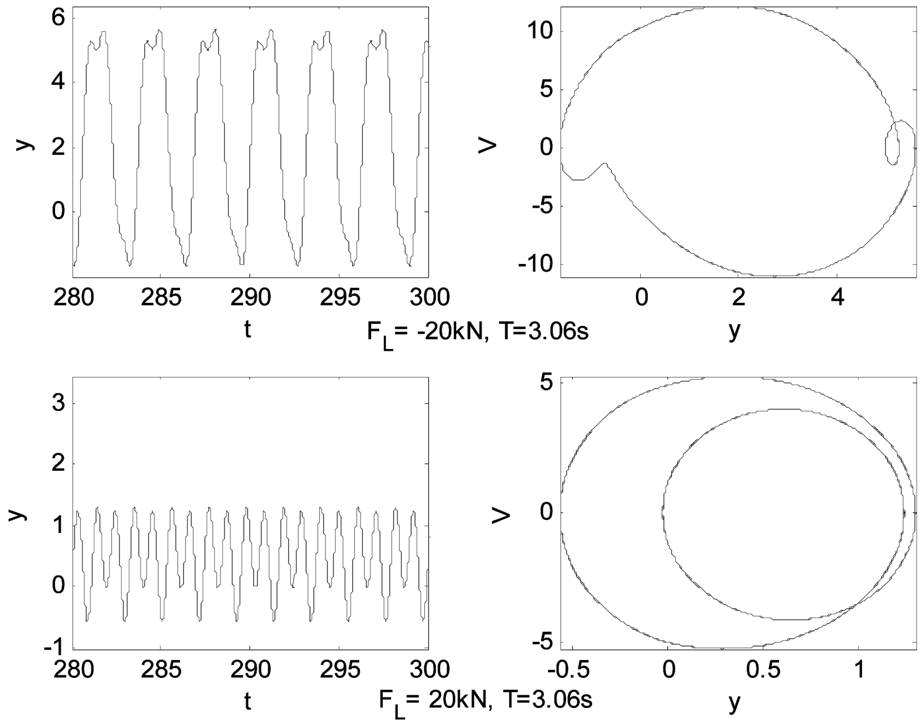

Fig. 21 Effect of sense of peak sinusoidal load F_2 on the steady state displacement response and phase plot of the system ($\beta = 8$, $\xi = 0.05$, $T = 3.06$ s)

almost identical systems lack any correlation. The above response has been computed for the system under the action of peak sinusoidal force of 20 kN. As can be observed from Fig. 19(b), the discontinuities in the system response vanish if the sense of the peak sinusoidal force is reversed. For the purpose of illustration, the displacement waveforms as well as the phase plots have been compared in Fig. 21 for the same structure with period equal to 3.06 s and under the action of positive and negative peak sinusoidal force. It has been confirmed that the presence or absence of the instabilities in the system response also depends considerably upon the sense of the peak sinusoidal force. However, the response of the system with period equal to 3.06 s under negative peak sinusoidal force is closer to the response of the system with period equal to 3.05 s with positive peak sinusoidal force. This fact is confirmed by their corresponding phase plots shown in Fig. 20 and Fig. 21. It has been verified that Model-II response also exhibits similar dependence on the period of the system as well as on the sense of the peak sinusoidal force

As is the case for general nonlinear systems, the principle of superposition can not be employed in the present case as well for obtaining the system response under combined loading by adding together the system response to constant sustained load and sinusoidal force separately. Because of this fact, the effect of constant sustained load on system response to sinusoidal force has been studied in a direct manner without invoking the superposition principle. It has been found that, in the present case, the presence of constant sustained load does not merely contribute to the system response, but it also alters considerably the nature of the dynamical system itself. Specifically, and significantly, as explained below, the presence of constant sustained load transforms the given time-invariant bilinear dynamical system into one which exhibits temporal evolution during vibrations.

It is well known that the natural time period of a dynamical system refers to the undamped system undergoing free vibrations (Chopra 1995, Clough and Penzien 1993, Humer 2002). Contrary to the linear SDOF dynamical systems, the bilinear SDOF dynamical systems stay in the positive vibration excursion for a different duration than in the negative vibration excursion. From the numerical specifications of the present system provided above, it is known that the undamped version of the system spends 0.1593314 s and 0.0563321 s in the positive and negative amplitude excursions respectively, thus resulting in its natural time period of 0.2156636 s. In the presence of constant sustained load introducing negative displacement, suppose the bilinear system, on being suitably perturbed from its equilibrium state, undergoes vibrations about the equilibrium state with positive as well as negative peak amplitudes. These peak vibration amplitudes gradually get damped out with this damped dynamical system asymptotically settling into the equilibrium state of rest of negative displacement. With each successive cycle, the system spends progressively lesser time in the positive excursion and, after the elapse of certain duration of time, both the peak amplitudes about the equilibrium state remain negative. Just after being perturbed, when the system exhibits relatively large positive vibration peak amplitude, the first vibration cycle is completed in a time period of about the damped period of 0.2156933 s of the system. The period of first cycle depends upon the magnitude of constant sustained load as well as of the perturbation. In contrast, finally the system settles into vibrations with negative peak amplitudes with the associated period of the cycle of 0.1128054 s which is independent of both the sustained load and the perturbation. Thus, the system executes vibration cycles in durations varying from about 0.2156933 s to 0.1128054 s.

As an illustrative example, the vibrations of the above dynamical system under the action of constant sustained load of −40 kN when perturbed from the equilibrium displacement of −0.016076 m by imparting an initial velocity of 10 m/s have been investigated. The resulting waveform, plotted in Fig. 22, confirms the above assertions. In particular, the first eight vibration cycles are executed in 0.185 s, 0.176 s, 0.166 s, 0.155 s, 0.140 s, 0.131 s, 0.121 s and 0.1128 s respectively. These vibration periods have been determined as the time lapse between the successive negative peak

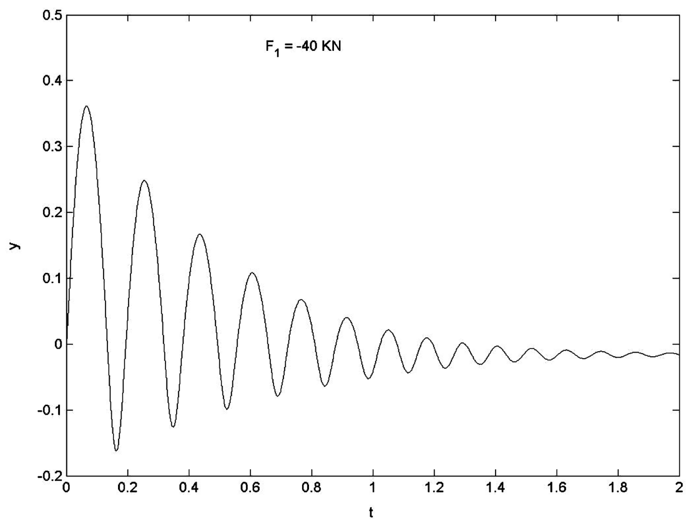

Fig. 22 Displacement responses for free vibration (F_1= −40 kN)

amplitudes. After the eighth cycle, the vibration amplitude can be observed to remain negative. It is understood, of course, that the above effect of the presence of dead load on vibration cycle period pertains only to damped systems, whereas undamped systems do not exhibit such an effect. Also, the dynamical systems with higher damping ratio are expected to experience change in period---from 0.2156933 s to 0.1128054 s in the above example---in lesser number of cycles. This illustrative example pertains to Model-III, but similar behavior is also expected from Model-II of the bilinear dynamical system.

Under the combined action of constant sustained load and sinusoidal force, the bilinear systems asymptotically exhibit steady state vibrations after the transient vibrations have been damped out. For these bilinear systems, these steady state vibrations may be executed at frequencies other than the forcing frequency. As argued above, the period of these steady state vibrations is determined by the durations of positive and negative excursions of the system which, in turn, are determined by the system parameters, relative magnitudes of constant load and sinusoidal force, and the forcing frequency. The same very factors determine the 'natural' period as well as frequency of the bilinear systems. Thus, in the presence of constant load, the 'natural' frequency of the bilinear systems is not definitely known. Resonance occurs as and when the forcing and the 'natural' frequencies match. Because of the fact that the constant load affects the 'natural' frequency of the bilinear system, the resonance is expected to occur at forcing frequencies depending upon the magnitude of the sustained constant load.

The effect of constant sustained load on the forced vibrations of bilinear dynamical systems has been studied with peak amplitude of sinusoidal force F_2 as -20 kN and for various values of constant sustained load F_1. The frequency domain response of the system for positive and negative peak amplitudes has been plotted in Fig. 23 and Fig. 24 for load ratios (F_1/F_2) of 0, 1, 2, 3, ..., 10. The sub-harmonics have been observed to vanish at quite low values of constant load. The peak positive fundamental response keeps on deceasing continuously with increase in constant sustained load. In contrast, the absolute value of the peak negative fundamental response first decreases and then starts increasing after reaching a minimum value at a load ratio of about two. Also, with increase in constant load, the positive as well as negative peak fundamental response has been

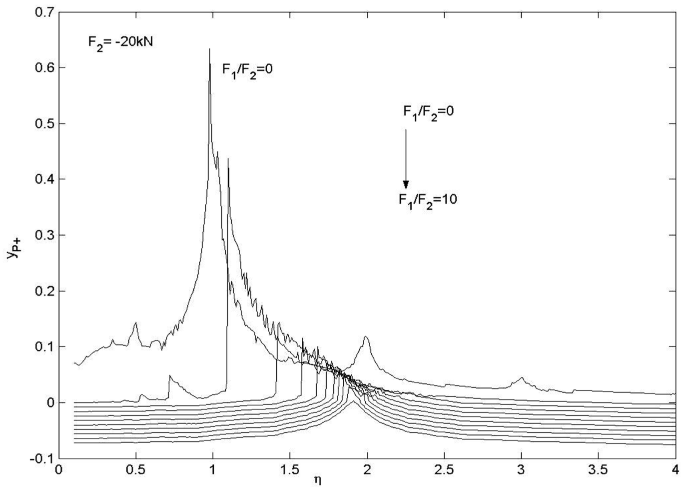

Fig. 23 Frequency domain plot for peak positive resonance response

observed to occur at higher values of the frequency ratio, and so of the forcing frequency. In the absence of constant load, the fundamental peak response is known to occur at a frequency ratio of unity. In contrast, for very high values of load ratio---exceeding about 9.13 in the present case---the system becomes linear with the natural frequency (ω_2) of 55.769 rad/s and the corresponding frequency ratio of 1.91. It is worth recapitulating here that the frequency ratio in the present context represents the ratio of the forcing frequency to the natural frequency (ω_n = 29.134 rad/s) of the corresponding undamped bilinear system in the absence of constant load. Thus, as the load ratio increases from 0 to 10, the resonance occurs at the corresponding frequency ratios varying from 0.98 to 1.91. At higher load ratios, the resulting linear dynamical system exhibits resonance at the same frequency ratio of 1.91.

The effect of load ratio on the frequency ratio at resonance pertaining to fundamental peak positive response has been shown in Fig. 25. In contrast to the conventional linear SDOF systems,

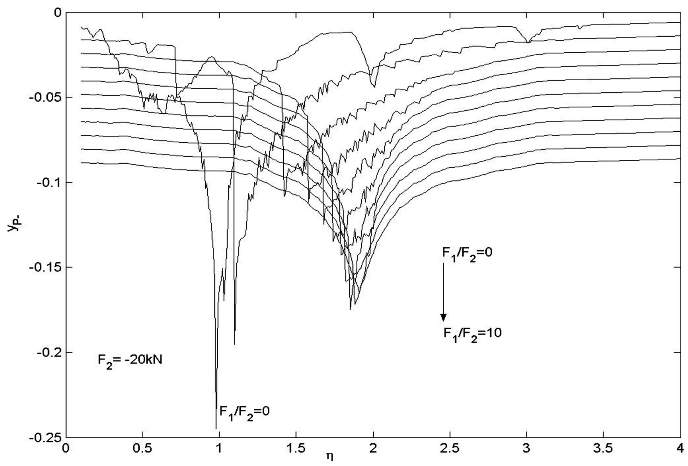

Fig. 24 Frequency domain plot for peak negative resonance response

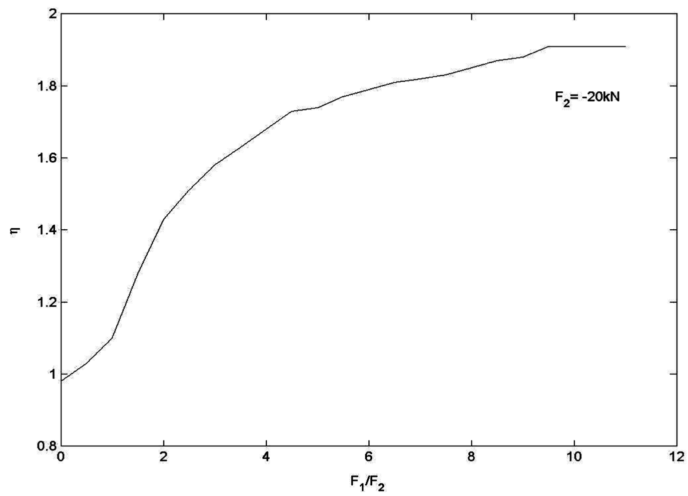

Fig. 25 Frequency ratio for fundamental peak positive displacement vs load ratio

the frequency ratio at resonance for the bilinear systems under the action of dead load differs from unity. It can be observed that the fundamental resonance frequency ratio increases with load ratio, the rate of increase being higher at lower load ratios. The rate of increase of resonance frequency ratio decreases gradually at higher load ratios. The maximum value being attained is 1.91 at a load ratio of 9.13. At still higher load ratios, such an effect is altogether absent.

The effect of constant sustained load on the frequency domain response of the bilinear systems to sinusoidal force without the constant sustained load has been presented above. The effects on the displacement, velocity and acceleration waveforms for Model-III have been presented in Fig. 26 and the corresponding steady state phase diagrams have been plotted in Fig. 27. The system response to the simultaneously acting constant and sinusoidal forces has been obtained at a frequency ratio of 0.98 and the load ratio of unity. The conclusions drawn from the frequency domain response are confirmed. For the particular case studied, the presence of constant load results in a substantial decrease (about twenty times) in the peak velocity and acceleration response. So far as the peak amplitude response is concerned, the positive amplitudes vanish and the vibration excursions remain in the negative amplitude side, even though the negative peak amplitude response has also been suppressed. In fact, for the particular structure studied, the constant load has the effect of pushing the phase diagram entirely to the negative amplitude side. This seems to be because of the fact that the applied constant load introduces negative static displacement in the structure. The presence of constant load can be observed to have considerable effect on the phase plot as shown in Fig. 27. The above conclusions are not applicable in general but only for the chosen forcing frequency corresponding to the peak fundamental response. The effect of constant load is expected to be different at some other forcing frequency.

In the above computational study, the constant sustained load has been taken to be different from

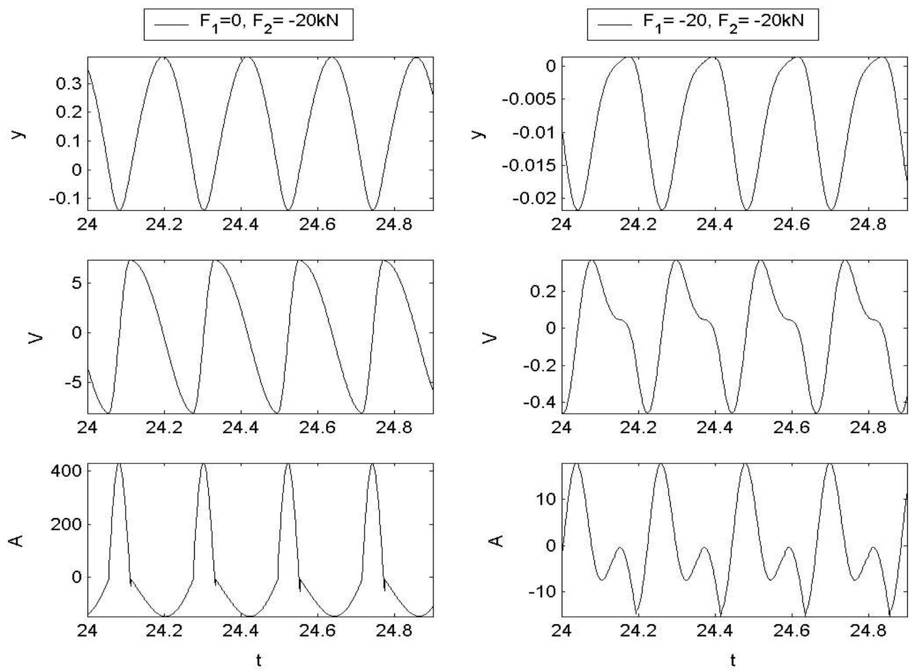

Fig. 26 Effect of constant sustained load on response of Model-III (F_2 = –20 kN)

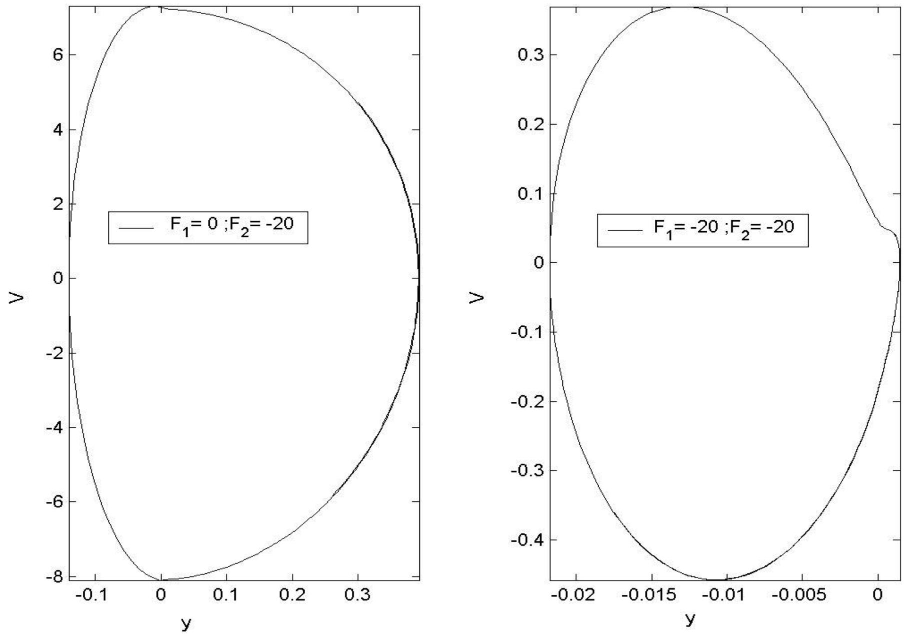

Fig. 27 Effect of constant sustained load on phase plot of Model-III (F_2 = –20 kN)

the weight of the vibrating mass. Of course, the procedure adopted is capable of dealing with the special case when the self weight constitutes the only constant sustained load as is the case for most of the structures.

5. Critical evaluation of proposed theory

The practical relevance of the results obtained for structural design as well as the theoretical significance of the approach followed in this paper is discussed below:

In conjunction with the authors' paper (Pandey and Benipal 2006), the present paper constitutes the very first attempt dealing with the dynamic response of SDOF cracked concrete structures under working loads. It is not clear whether these bilinear dynamical systems are characterized by their damping coefficient or damping ratio. The Model-II investigated earlier presumes constant damping coefficient, while the Model-III studied in this paper is based on the assumption of constant damping ratio. The elastodynamical behavior of Model-III to sinusoidal loading has been investigated in this paper and has been compared with Model-II used earlier by the authors (Pandey and Benipal 2006) to simulate the behavior of cracked concrete structures. It has been found that the Model-III also exhibits, like Model-II, regular and irregular sub-harmonics and strong sensitivity to initial conditions. However, it does not exhibit simultaneous over/underdamped response. Model-III is characterized by jump phenomena in its waveforms for acceleration response as well as in its waveforms for damping force and inertial force. Like any sound theory, these two models suggest an experimental procedure for checking whether the actual cracked concrete structures are characterized by their damping coefficient or damping ratio. It has been established that strong discontinuities are present in the dependence of Model-III response on forcing frequency, natural period of the structure and sense of the peak sinusoidal force. It has been verified that, qualitatively, such is the case with Model-II as well.

Some experimental evidence is available which implies that the damping ratio of concrete beams increases with the extent of damage in the form of flexural cracks (Chung *et al*. 1999, Salzman 2003, Demaric and Sabia 2011). It seems that the reduction in stiffness due to the presence of cracks results in the reduction of the critical damping coefficients. If the damping coefficient is assumed to be constant, as in Model II, the damping ratio of the cracked concrete beams is indeed expected to be higher. However, as mentioned earlier, as per the current practice in structural dynamics, steel and concrete structures are assigned their characteristic damping ratio. It has been observed (Demaric and Sabia 2011) that even the Rayleigh damping model popular among structural engineers is at variance with experimental data. Also, apart from the two conventional damping modes, i.e., over and under damping modes, concrete structures have been found to exhibit third damping mode, To model such observed behavior, a third order linear differential equation of motion incorporating the effect of rate of loading has been proposed (de Haan and Sluimer 2001). Obviously, the issue of damping of vibrations in concrete structures has not yet been resolved. As of now, the issue of establishing relative merits of Model II and Model III remains unresolved.

The service loads acting on the concrete structures have a constant component, usually self weight of the structure, and a variable live load component. The latter component has been modeled here as sinusoidal loading. The effect of constant load on the behavior of different models of cracked concrete structures subjected to sinusoidal loading has been investigated in this paper. Apart from shifting the equilibrium state and so affecting the system response, it has been established that, in the presence of constant load, the period of damped structures simulated by Model-III varies with passage of time resulting in gradual change in their ‘natural’ frequency and so their resonance frequency. Though the sub-harmonics and the fundamental positive peak response are suppressed by the presence of negative constant sustained load, the fundamental negative peak response gets enhanced. The magnitude of these fundamental peak responses depend upon the load ratio. It has been established that these fundamental peaks do not occur at a frequency ratio of unity but at a resonance frequency ratio determined by the load ratio. These conclusions are of tremendous importance in the analysis and design of concrete structures under service loads.

The results obtained in this paper are of tremendous significance for dynamic analysis, design, control, health monitoring, retrofitting and system identification of concrete structures. Also, in contrast to the linear dynamical systems, the bilinear systems have been shown to execute steady state vibrations at frequencies different from the forcing frequency. The elastodynamic response of concrete structures subjected to sinusoidal forcing so determined is expected to be useful for ensuring their safety under general dynamical loading and, in particular, earthquakes of magnitude lower than the design earthquakes. Also, the magnitude of the seismic forces acting on properly controlled structures is expected to be such as not to introduce any inelastic behavior even though the concrete structures may still be cracked. Similarly, the procedure for health monitoring and system identification of in-service concrete structures involves the determination of their elastodynamic response to applied sinusoidal loading of small magnitude. In view of these facts, the significance of the proposed theory for predicting their elastic response becomes obvious. To be specific, concrete beams with breathing cracks have been shown to exhibit subharmonic resonances at higher forcing frequencies thus confirming their observed behavior (Bayissa and Haritos 2004). In this context, it is also significant to note that, like typical nonlinear systems, cracked concrete beams also exhibit splitting of resonance response peaks into two or more resonance peaks with different amplitudes occurring at adjacent forcing frequencies. Contrary to popular perception in damage detection investigations, the dead load itself as well as the relative magnitude of applied peak sinusoidal force and dead load has been predicted to have considerable effect on the dynamic behavior. It is worth remembering that the available experimental data pertains to concrete beams with distributed mass, while the scope of present study is limited to lumped mass SDOF beams.

Even when the concrete structures exhibit elastoplastic behavior under the action of strong earthquakes, the peculiar dynamic effects associated with different stiffness and damping coefficients depending upon the sense of amplitude are not expected to vanish. In particular, as is the current practice, the passive control of vibrations aims at avoiding fundamental resonant peaks by suitable selection of system stiffness. Usually, this aim is achieved by choosing more flexible structure. The presence of subharmonic resonances predicted for cracked concrete beams can render the above passive control strategy useless. This is because of the fact, as shown in Fig. 6, that the predicted subharmonic peak response of the flexible structure can be as high as the fundamental peak response being controlled. The dynamic response of flexible structures predicted by following the current practice of assuming gross stiffness will underestimate the actual subharmonic peak response by a factor of 2 to 3. Similarly, the ever-present noise in the waveforms obtained from dynamical testing of actual structures for health monitoring, system identification and retrofitting purposes is not entirely due to measurement errors. It could well be the result of subharmonics and sensitivity of structural response to various details of structure and loading.

For simplicity of analysis, the proposed Model-I of the bilinear oscillator treats the cracked concrete structures as equivalent unilinear dynamical systems without changing their natural period. As per the current design practice, the presence of cracking and reinforcement is ignored. Obviously, the inadequacies of the approximate linear dynamical analysis procedures adopted by the designers are revealed. However, as expected, these linear oscillators do not exhibit the above complexities of dynamical response associated with bilinear oscillators.

The theoretical significance of the present study can be realized by comparing the governing differential equations of the Model-II and Model-III SDOF oscillators with the well known SDOF Duffing and van der Pol oscillators (Thompson and Stewart 1986). The SDOF dynamical systems have also been employed to model oscillators with clearances (Hossain *et al*. 2002, Natsiavas 1990). The special case pertaining to no clearance or gap assigns two different values to stiffness and damping coefficients depending upon the sense of the amplitude resulting in two unrelated damping ratios. Of course, the formulation reduces to Model-II or Model-III of the present investigation respectively when the damping coefficients or damping ratios are assigned constant value independent of the sense of the amplitude. It should be mentioned here that, in these investigations focusing on the general model, the Model-II and Model-III have not been studied in any detail as special cases.

To recapitulate, the experimental investigations on the dynamical behavior of cracked concrete beams have predominantly been carried out by researchers primarily interested in damage detection for structural health monitoring. Only those linear dynamic characteristics, like natural frequencies, which can be employed for quantification of damage, are measured. Sometimes, other nonlinear dynamical characteristics like shift in fundamental resonance frequency due to cracking, jump phenomenon associated with increasing/decreasing forcing frequency, etc., are also employed for the same purpose. Subharmonics and sensitivity to initial conditions exhibited by cracked concrete beams have not yet attracted the attention of these researchers. Even the bilinear nature of the cracked beam cross-section has only recently been recognized. It should also be realized that concrete beams used in these experimental investigations have distributed mass with infinite degrees of freedom. Also, the tested concrete beams undergo inelastic cracking during vibrations. In contrast, the present paper deals with the fully cracked SDOF elastic concrete beams.

Thus, the experimental data relevant for empirical validation of the proposed model is not available. It is claimed here that, in this paper, even such a simple structure as a SDOF cracked concrete beam has been predicted to exhibit very complex and interesting dynamical behavior. Real concrete structures in the laboratory or in the field are expected to display unexpected dynamical behavior.

6. Conclusions

The present paper along with authors' earlier paper constitutes the first exhaustive study on the dynamic behavior of SDOF elastic cracked concrete structures under service loads modeled as bilinear dynamical systems. In the present paper, three different models of these bilinear dynamical systems have been proposed.

The elastodynamics of Model-III under sinusoidal load has been investigated and compared with Model-II investigated earlier. Both the models have been shown to exhibit regular and irregular sub-harmonics and sensitivity to initial conditions. Model-III lacks simultaneous over/underdamped response but exhibits distinctive jump phenomena and sensitivity to system parameters like natural period but only for positive peak sinusoidal force. The Model-I has been shown to be more realistic than the method followed in practice for analyzing concrete structures.

The effect of constant sustained load on the dynamic response of different models subjected to sinusoidal load has also been presented. It has been found that, in the presence of constant load, the Model-II and Model-III are transformed into time-variant systems.

The practical implications of the work done for the analysis, design and testing of concrete structures under working loads have been pointed out. In contrast to the all-inclusive scope of the contemporary research papers, the present paper has very limited scope. Obviously, because of the approach followed, it has been possible to employ, for the first time, the concepts and techniques of nonlinear dynamical systems theory to study the dynamical behaviour of the elastic cracked concrete structures and thereby predicting some hitherto-unknown aspects of their dynamic behavior. The three models of bilinear oscillators proposed in this paper are also claimed to constitute a definite contribution to the general nonlinear dynamical systems theory.

References

Agarwal, P. and Shrikhande, M. (2006), *Earthquake Resistant Design of Structures*, Prentice Hall of India Private Ltd., New Delhi.

Bayissa, W.L. and Haritos, N. (2004), "Experimental investigation into vibration characteristics of a cracked T-beam", *Proceedings of the Conference of Australasian Earthquake Engineering Society*, Mt. Gambier, South Australia.

Benipal, G.S. (1994), "Rational mechanics of reinforced concrete beams", *Proceeding National Symposium on Structural Mechanics*, I.I. Sc. Bangalore, India, June.

BIS-IS: 1893-2002: Indian Standard Code of Practice-criteria for Earthquake Resistant Design of Structures,

Bureau of Indian Standards, New Delhi.
BIS-IS: 456-2000: Indian Standard Code of Practice for Plain and Reinforced Concrete, Bureau of Indian Standards, New Delhi.
Carrión, F.J., Lozano, A. and Castaño, V.M. (2006), "Condition monitoring of vibrating steel-reinforced concrete beams through wavelet transforms", *Struct. Surv.*, **24**(2), 154-162.
Chen, G., Yang, X., Ying, X. and Nanni, A. (2006), "Damage detection of concrete beams using nonlinear features of forced vibration", *Struct. Hlth. Monit.*, **5**(2), 125-141.
Chopra, A.K. (1995), *Dynamics of Structures*, Prentice-Hall of India, New Delhi.
Clough, R.W. and Penzien, J. (1993), *Dynamics of Structures*, McGraw Hill, Singapore.
Chung, Y.S., Park, Y.G., Cho, S.H. and Lee, K.M. (1999), "Experimental study on the dynamic characteristics of a vibration controlled concrete beam", *Proceedings of the 15th International Conference on Structural Mechanics in Reactor Technology* (SMIRT 15) Held at Seoul, Korea, August.
de Haan, Y.M. and Sluimer, G.M. (2001), "Standard linear solid model for dynamic and time dependent behavior of building material Heron", *Heron,* **46**(1), 49-76.
Demaric, G.V. and Sabia, D. (2011), "Non-linear damping and frequency identification in a progressively damaged R.C. element", *Exper. Mech.*, **51**(2), 229-245.
Eccles, B.J., Owen, J.S., Choo, B.S. and Woodings, M.A. (1999), "Nonlinear vibration of cracked reinforced concrete beams", *Proceedings of the 4th Conference of European Association of Structural Dynamics* (EURODYN), Prague, Czechoslovakia.
Hossain, M.Z., Mizutani, K. and Sawai, H. (2002), "Chaos and multiple periods in an unsymmetrical spring and damping system with clearance", *J. Sound Vib.*, **250**(2), 229-245.
Humar, J.L. (2002), *Dynamics of Structures*, A.A. Balkema Publishers, Tokyo.
Huszar, Z. (2008), "Vibrations of cracked reinforced and prestressed concrete beams", *Arch. Civil Eng.*, **6**(2), 155-164.
Musial, M., Kaminski, M. and Ubysz, A. (2009), "Free vibration frequencies of the cracked reinforced concrete beams-Methods of calculations", *Proceedings of the 18th International Conference on the Application of Computer Science and Mathematics in Architecture and Civil Engineering*, (Eds. K. Gürlebeck and C. Könke), Weimar, Germany, July.
Natsiavas, S. (1990), "On the dynamics of oscillators with bilinear damping and stiffness", *Int. J. Nonlin. Mech.*, **25**(5), 535-554.
Ndambi, J.M., Peeters, B., Maeck, J., De Visscher, J., Wahab, M.A., De Roeck, G. and De Wilde, W.P. (2000), "Comparison of techniques for modal analysis of concrete structures", *Eng. Struct.,* **22**(9), 1159-1166.
Neild, S.A., Williams, M.S. and McFadden, P.D. (2003), "Non-linear vibration characteristics of damaged concrete beams", *J. Struct. Eng.-ASCE,* **129**(2), 260-268.
Newtson, C.M., Gaur, P.J. and Brian, T.E. (2006), "Fundamental frequency testing of reinforced concrete beams", *J. Perform. Constr. Fac.,* **20**(2), 196-200.
Pandey, U.K. and Benipal, G.S. (2006), "Bilinear dynamics of SDOF concrete structures under sinusoidal loading", *Adv. Struct. Eng.*, **9**(3), 393-407.
Pandey, U.K. (2008), "Nonlinear elastodynamics of cracked concrete beams", PhD Thesis submitted at Indian Institute of Technology Delhi, New Delhi.
Pauley, T. and Priestley, M.J.N. (1982), *Seismic Design of Reinforced Concrete and Masonry Buildings*, John Wiley & Sons, New York.
Penelis, G.G. and Kappos, A.J. (1997), *Earthquake Resistant Concrete Structures*, E & FN SPON, London.
Salzman, A., Fragomeni, S. and Loo, Y.C. (2003), "The damping analysis of experimental concrete beams under free-vibration", *Adv. Struct. Eng.,* **6**(1), 53-64.
Teguh, M., Saleh, F., Duffield, C.F. and Hutchinson, G.L. (2006), "Strength deterioration of nonprismatic reinforced concrete beams", *Proceeding of first International Conference on Computational Methods (ICCM04),* held at Singapore, Springer, 1805-1815.
Thompson, J.M.T., Bokaian, A.R. and Ghaffari, R. (1983), Sub-harmonic and chaotic motions of a bilinear oscillator", *IMA J. Appl. Math.*, **31**, 207-234.
Thompson, J.M.T., Bokaian, A.R. and Ghaffari, R. (1984), "Sub-harmonic and chaotic motions of compliant offshore structures and articulated mooring towers", *ASME J. Energy Resour. Tech.,* **106**, 191-198.

Thompson, J.M.T. and Elvey, J.S.N. (1984), "Elimination of sub-harmonic resonances of compliant marine structures", *Int. J. Mech. Sci.*, **26**, 419-425.
Thompson, J.M.T. and Stewart, H.B. (1986), *Nonlinear Dynamics and Chaos*, John Wiley and Sons, New York.
Wang, Z., Man, X.C., Finch, R.D. and Jansen, B.H. (1998), "The dynamic behavior and vibration monitoring of reinforced concrete beams", *J. Test. Eval.,* ASTM, **26**(5), 405-419.
Zhu, X.Q. and Law, S.S. (2007), "Nonlinear characteristics of damaged reinforced concrete beam from Hilbert-Huang transform", *J. Struct. Eng.-ASCE,* **133**(8), 1186-1191.
Zhu, X.Q., Law, S.S. and Hao, H. (2009), "Damage assessment of reinforced concrete beams including the load environment", *Struct. Eng. Mech.,* **33**(6), 765-779.

Notations

A : Acceleration (m/s^2)
c : Damping coefficient (N-s/m)
C_{cr} : Critical damping coefficient
f_{ck} : Characteristic strength of concrete (N/mm^2)
Ec : Modulus of elasticity of concrete
F_1, F_o : Constant sustained load (N)
F_2, F_L : Peak Sinusoidal force (N)
F_D : Damping force (N)
F_E : Elastic force (N)
F_{In} : Inertial force (N)
k : Stiffness values (N/m)
K : Averaged stiffness (N/m)
m : Lumped mass (kg)
n : Order of the sub-harmonics
P : Percentage of steel
t : Time (s)
T : Natural period (s)
T_D : Damped period (s)
V : Velocity (m/s)
V_s : Initial velocity (m/s)
$y, \dot{y}, \ddot{y}$: Displacement, velocity and acceleration
y_{P-} : Maximum negative peak amplitude (m)
$|y_{P-}|$: Absolute value of maximum negative peak amplitude (m)
y_{P+} : Maximum positive peak amplitude (m)
β : Bilinearity ratio (k_2/k_1)
ξ : Damping ratio
η : Frequency ratio (ω_f/ω_n)
ω_D : Damped frequency (rad/s)
ω_f : Forcing frequency (rad/s)
ω_n : Bilinear natural frequency (rad/s)

N.B. The symbols (c, K, k, P, y, ω_D, ω_n and ξ) with subscript 1 refer to the case when the top reinforcement P_1 is in tension and the same symbols with subscript 2 refers to the case when the bottom reinforcement is in tension.